# UNIVERSITÄTSKLINIKUM HAMBURG-EPPENDORF

Klinik und Poliklinik für Allgemeine und Interventionelle Kardiologie
Universitäres Herzzentrum Hamburg

Prof. Dr. med. Stefan Blankenberg

## Analysis of AGAT-related mRNA and miRNA expression in the murine heart

**Dissertation**

zur Erlangung des Grades eines Doktors der Medizin
an der Medizinischen Fakultät der Universität Hamburg.

vorgelegt von:

Märit Jensen
aus Hamburg

Hamburg 2018

Angenommen von der
Medizinischen Fakultät der Universität Hamburg am: 25.03.2019


Veröffentlicht mit Genehmigung der
Medizinischen Fakultät der Universität Hamburg.


Prüfungsausschuss, der/die Vorsitzende:     Prof. Dr. Tanja Zeller


Prüfungsausschuss, zweite/r Gutachter/in:   Prof. Dr. Viacheslav Nikolaev

# Table of contents

# 1 Introduction

## 1.1 Cardiovascular disease

Cardiovascular disease (CVD), including disorders of the heart and the circulatory system, represents the leading cause of death in Europe. According to the European Society of Cardiology, more than 4 million Europeans die of CVD every year (45% of all deaths) (Townsend et al., 2016). The main form of CVD is coronary artery disease (CAD), in which atherosclerotic narrowing of arteries results in insufficient blood supply of the heart. This manifests itself as angina or myocardial infarction (MI), which, over time, may lead to heart failure (Hansson, 2005).

The majority of CVD is caused and aggravated by classical risk factors, such as hypertension, cigarette smoking, hypercholesterolemia, obesity and diabetes mellitus (Moran et al., 2014). Several pharmacological interventions to address and manage these risk factors are available, however, some patients do not benefit from common medication. Therefore, a major scientific and clinical aim is to identify novel biomarkers and genetic variants that might influence CVD outcome. To this end, further investigations to understand the underlying metabolic pathways and molecular mechanisms are needed to develop novel diagnostic and therapeutic strategies (Lewis et al., 2008, Lloyd-Jones, 2010).

One of the main reasons for CVD is atherosclerosis and it is assumed that a potential cause for the development of atherosclerosis is insufficient formation of nitric oxide (NO). Latest research shows that the L-arginine derivative homoarginine is involved in NO metabolism and predicts the prognosis of cardiovascular patients (Choe et al., 2013a, Gore et al., 2013, Atzler et al., 2013). The responsible enzyme is L-arginine:glycine amidinotransferase (AGAT), for which reason the further characterization of this metabolic pathway is of particular interest.

## 1.2 L-arginine:glycine amidinotransferase

The enzyme L-arginine:glycine amidinotransferase (AGAT; EC: 2.1.4.1) is encoded by the *AGAT* gene and belongs to the amidinotransferase family (NCBI Gene) (Brown et al., 2015). In recent years, AGAT has gained in importance in cardiovascular research since it is not only responsible for the synthesis of the cardiac energy buffer creatine, but also involved in the formation of the cardiovascular risk marker homoarginine (Choe et al., 2013a). The molecular connection of AGAT and homoarginine has been shown in genome-wide association studies (GWAS), since homoarginine plasma levels are associated with genetic variations within the *AGAT* gene (Choe et al., 2013a, Kleber et al., 2013). *In vitro* studies showed that synthesis of homoarginine was not detectable in AGAT-deficient lymphoblasts (Davids et al., 2012). Consistently, AGAT-deficient mice revealed undetectable homoarginine levels as evidence of homoarginine formation by AGAT *in vivo* (Choe et al., 2013a).

The enzymatic reaction of AGAT is illustrated in Figure 1. Creatine synthesis is a two-step process consisting of AGAT and guanidinoacetate N-methyltransferase (GAMT; EC 2.1.1.2). In a first step, AGAT transfers an amidino group from L-arginine to glycine to form guanidinoacetic acid (GAA). The second step is catalyzed by GAMT and includes the methylation of GAA resulting in creatine.

Besides the formation of creatine, AGAT is also involved in homoarginine synthesis. Here, AGAT catalyzes the addition of the amidino group of L-arginine to lysine to form homoarginine (Atzler et al., 2015).
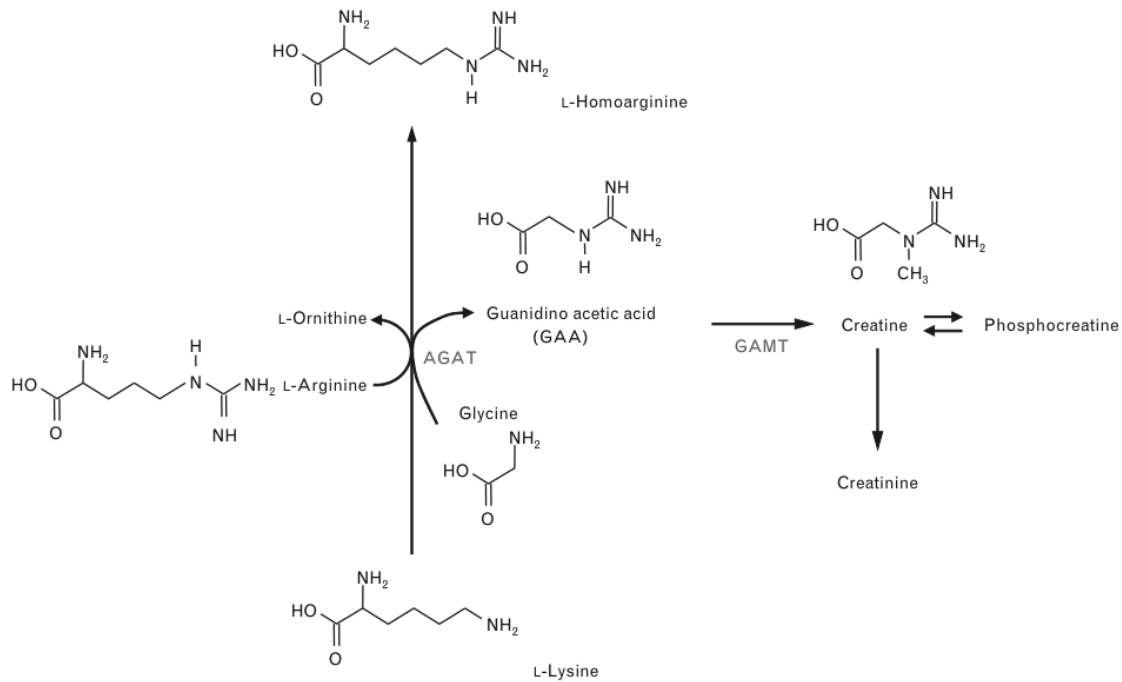
**Figure 1: Scheme of creatine and homoarginine synthesis**
L-arginine:glycine amidinotransferase (AGAT) transfers the amidino group of L-arginine to glycine producing guanidinoacetic acid (GAA). Guanidinoacetate N-methyltransferase (GAMT) methylates GAA resulting in creatine formation. Homoarginine synthesis involves AGAT, which transfers the amidino group of L-arginine to lysine, producing homoarginine. Figure from Atzler et al., 2015, Figure 1: Scheme of creatine and homoarginine metabolism.

The major sites of endogenous creatine biosynthesis are the pancreas, kidneys and liver, where AGAT is located in the cytoplasm and in the intermembrane space of the mitochondria (Humm et al., 1994). In accordance, *AGAT* mRNA is highly expressed in human kidneys and liver. Furthermore, AGAT is expressed in tissues with high energy demand such as striated muscle, heart and brain (Braissant and Henry, 2008, Cullen et al., 2006). Studies have demonstrated that AGAT activity in these tissues is regulated in several ways, including a repression of its synthesis by creatine as a feedback mechanism (McGuire et al., 1984, Guthmiller et al., 1994), inhibition by the non-proteinogenic amino acid ornithine and induction of the enzyme by growth hormone and thyroxine (Sipilä, 1980). Moreover, it has been described that sex hormones such as testosterone or estrogen might regulate the expression and activity of AGAT (Krisko and Walker, 1966, Zhu and Evans, 2001).

### 1.2.1 Creatine

The primary product of AGAT, the nitrogenous organic acid creatine plays a pivotal role in vertebrate energy metabolism. After synthesis of creatine, especially in the pancreas, kidneys and liver, it is transported through the blood towards organs with high energy demands such as skeletal muscle, brain and heart tissue (Nabuurs et al., 2013). Here, the creatine/phosphocreatine (PCr) system is involved in the recycling of adenosine triphosphate (ATP), which is an important source of energy for the cell. In brief, the enzyme creatine kinase (CK) catalyzes the donation of phosphate groups from PCr to adenosine diphosphate (ADP) through a reversible reaction: Creatine + ATP $\leftrightarrow$ PCr + ADP (Wyss and Kaddurah-Daouk, 2000). A proportion of about 1.5% of total creatine is degraded non-enzymatically into creatinine and finally eliminated by renal excretion (Nabuurs et al., 2013). Diseases induced by creatine deficiency mainly manifest in organs with high energy demands, especially skeletal muscle and brain with muscular hypotonia and mental retardation (Stockler et al., 1996, Item et al., 2001, Stockler et al., 2007).

### 1.2.2 Homoarginine

The AGAT-derived metabolite homoarginine is a non-proteinogenic and endogenous amino acid that only differs from L-arginine by an additional methylene group (Jazwinska-Kozuba et al., 2013). First studies about its physiological function revealed that homoarginine inhibits human liver and bone alkaline phosphatase (Lin and Fishman, 1972). More recent, studies showed an involvement of homoarginine in vascular and endothelial function. Given its structural similarity to L-arginine, homoarginine is suspected to interfere with L-arginine pathways. L-arginine serves as a substrate for NO synthesis and NO itself is a powerful vasodilator with a short half-life time of a few seconds in the blood (Röszer, 2012). Several studies revealed that homoarginine can serve as an alternative substrate for NO synthase (NOS) (Moali et al., 1998, Hrabak et al., 1994). Moreover, homoarginine was found to inhibit the enzyme arginase, thereby increasing L-arginine levels and in turn support NO production (Hrabak et al., 1994). In another study it has been demonstrated that homoarginine,

similar to L-arginine, inhibits aggregation of human platelets (Radomski et al., 1990).

## 1.3 Homoarginine in cardiovascular disease

### 1.3.1 Clinical impact

During the last years, epidemiological and clinical studies have shown that plasma homoarginine levels are associated with laboratory and clinical parameters in CVD and the outcome of patients (Choe et al., 2017). An overview is given in Figure 2. More precise, data from the LUdwigshafen RIsk and Cardiovascular Health (LURIC) Study and 4D study (Die Deutsche Diabetes Dialyse Studie) revealed an association of low homoarginine levels with increased cardiovascular and all-cause mortality (März et al., 2010). Consistently, findings from the Hoorn study confirmed that low homoarginine is a predictor of increased overall mortality and cardiovascular death in an elderly population (Pilz et al., 2014). In the LURIC study, analysis of the subtypes of cardiovascular death showed an association of low homoarginine plasma levels with fatal stroke (Pilz et al., 2011b). In addition, low homoarginine was associated with an increased risk of sudden cardiac death or death due to heart failure in the 4D study (Drechsler et al., 2011). It is undermining the role of homoarginine in heart failure that plasma homoarginine is associated with laboratory parameters such as natriuretic peptide blood levels (e.g. NT-proBNP) and left ventricular ejection fraction, showing a positive correlation between homoarginine and cardiac function (Drechsler et al., 2011, Pilz et al., 2011a). In line with these findings, the correlation between NT-proBNP levels and homoarginine could be demonstrated in another cohort of heart failure patients (Atzler et al., 2013). This study additionally showed that homoarginine levels are associated with clinical stages of heart failure. Patients suffering from moderate or severe heart failure (i.e. New York Heart Association classifications [NYHA] 3 and 4) exhibited decreased homoarginine levels (Pilz et al., 2011a, Atzler et al., 2013). Several studies suggested a link between a worsening of endothelial function and myocardial dysfunction. In this context, it has been reported that homoarginine is inversely associated with markers of endothelial function such as intercellular adhesion molecule-1 and vascular cell adhesion molecule-1 (März et al., 2010).

| Low homoarginine plasma levels |
| :---: |

| Laboratory and clinical parameters | Clinical outcome |
| :---: | :---: |
| NYHA stages[1,2] ↑ | All-cause and CV mortality[3,4] ↑ |
| NT-proBNP[2] ↑ | Fatal stroke[5] ↑ |
| Left ventricular ejection fraction[1] ↓ | Death due to heart failure[6] ↑ |
| | Sudden cardiac death[6] ↑ |
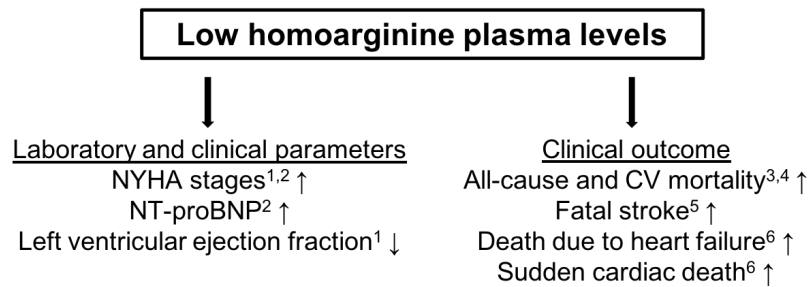
**Figure 2: Overview about the correlation of homoarginine plasma levels with laboratory and clinical parameters and clinical outcome in current studies**
An up arrow indicates an increase and a down arrow a decrease of the corresponding parameter. NYHA: New York Heart Association classification; NT-proBNP: N-terminal prohormone of brain natriuretic peptide; CV: cardiovascular. References: [1]Pilz et al., 2011a; [2]Atzler et al., 2013; [3]März et al., 2010; [4]Pilz et al., 2014; [5]Pilz et al., 2011b; [6]Drechsler et al., 2011.

## 1.3.2 Experimental evidence

An AGAT-deficient (AGAT$^{-/-}$) mouse model has been established in order to evaluate AGAT-dependent metabolic and cardiovascular changes and to differentiate effects that are related to homoarginine or creatine (Choe et al., 2013b). First investigations regarding the metabolic phenotype demonstrated that AGAT deficiency in mice results in mitochondrial dysfunction and intracellular energy deficiency as well as structural and physiological abnormalities such as enhanced muscular atrophy and decreased grip strength. It has been shown that hind limb ischemia leads to a decrease of pH, indicating absence of an adequate buffering system and decreased tolerance to ischemia. These findings were completely reversible by creatine supplementation (Nabuurs et al., 2013). Another study showed that AGAT$^{-/-}$ mice exhibit significant metabolic changes such as reduced body weight and decreased fat deposition. Moreover, AGAT$^{-/-}$ mice showed signs of attenuated gluconeogenesis, improved glucose tolerance and lower cholesterol levels compared to wild-type (WT). Oral supplementation of creatine completely rescued the metabolic phenotype (Choe et al., 2013b). Regarding CVD, AGAT$^{-/-}$ mice revealed increased infarct sizes and aggravated neurological deficits after ischemic stroke. The supplementation with homoarginine but not creatine significantly reduced infarct size and prolonged survival (Choe et al., 2013a). Cardiac hemodynamic measurements in AGAT$^{-/-}$ mice showed low left ventricular (LV) systolic pressure and maximal heart rate in response to dobutamine infusion compared to WT. Moreover, a significantly impaired contractility (dP/dt$_{max}$), relaxation (dP/dt$_{min}$) and inotropic reserve has

been demonstrated in AGAT^{-/-} mice. Supplementation with homoarginine completely rescued all hemodynamic parameters, whereas dietary supplementation with creatine only corrected LV systolic pressure (Faller et al., 2017).

Since AGAT is responsible for the formation of creatine and homoarginine, it has to be considered that homoarginine might be only a marker of low intracellular creatine levels due to an impaired AGAT activity. For example in heart failure, low homoarginine levels might represent low creatine levels and thereby reduced intracellular energy stores in the failing heart (Lygate et al., 2013b). As described above, PCr serves as a rapidly available energy buffer in the heart and it has been demonstrated that key components of the creatine/PCr system are down-regulated in experimental induced heart failure models (Lygate et al., 2007). Creatine-deficient mouse models showed reduced inotropic reserve and increased susceptibility to cardiac ischemia injury (Spindler et al., 2004, ten Hove et al., 2005). Moreover, CK knockout mice revealed left ventricular hypertrophy and dilatation (Nahrendorf et al., 2005). However, increased creatine and PCr levels also resulted in left ventricular hypertrophy and myocardial dysfunction (Wallis et al., 2005). Furthermore, creatine-deficient mice showed an unaltered response to chronic MI (Lygate et al., 2013a). These studies suggest that the association of creatine and heart failure is more complex than presumed and that is even more the case for the role of homoarginine in CVD.

Taken together, clinical and experimental studies of AGAT and its metabolites homoarginine and creatine suggest a pivotal role of these molecules in CVD. Low homoarginine plasma levels are associated with poor clinical outcome. Of note, an impaired cardiac contractile function of AGAT^{-/-} mice was rescued by homoarginine supplementation. Furthermore, the supplementation with homoarginine in mice preserved cardiac function in experimental models of heart failure (Atzler et al., 2017). This leads to the hypothesis that oral supplementation of homoarginine presents a potential treatment for patients with CVD who are not benefiting from common medication. However, to date, the data on the underlying molecular mechanisms and pathways are scant.

# 2 Aims of the study

In the last years, low levels of circulating homoarginine emerged as an important cardiovascular risk factor. The responsible enzyme for endogenous homoarginine synthesis is AGAT, which is also involved in the synthesis of the cardiac energy buffer creatine. It has been shown that creatine deficiency leads to altered cardiac function in CVD. Since AGAT is responsible for the formation of both metabolites, it is of strong interest whether homoarginine is only a marker of low creatine levels or a causal mediator in CVD. AGAT$^{-/-}$ mice exhibit cardiac dysfunction that was corrected in part by creatine and totally by homoarginine supplementation. As the molecular mechanisms and transduction pathways within the AGAT metabolism still remain unclear, it was the overall aim of this study to gain insights into the molecular background. The specific aims were:

1. Identification of AGAT-related transcripts by using mRNA and miRNA expression analysis in relation to AGAT, homoarginine and creatine.

2. Identification of AGAT-related molecular pathways and candidate genes linking AGAT, homoarginine and creatine to CVD.

3. Identification of potential regulatory mechanisms of miRNAs on AGAT-related transcripts.

# 3  Materials

## 3.1  Antibodies

| | |
|---|---|
| Anti-p21/WAF1/Cip1, monoclonal | Merck Millipore |
| Anti-CTGF, polyclonal | Abcam |
| Anti-GAPDH, monoclonal | Cell signaling Technology |
| Anti-UCP2, polyclonal | Biolegend |
| Anti-mouse IgG | Vector Laboratories |
| Anti-rabbit IgG | Vector Laboratories |

## 3.2  Chemicals

| | |
|---|---|
| 2-Mercaptoethanol | Sigma Aldrich |
| 40% Acrylamid | Bio-Rad |
| 4x Laemmli sample buffer | Bio-Rad |
| Ace Glow PeqLab | PeqLab |
| Ammonium persulfate (APS) | Roth |
| Aqua dest. | Braun |
| Bovine serum albumin (BSA) | Serva |
| Bradford reagent | Bio-Rad |
| Bromphenol blue | Merck Millipore |
| Cell lysis buffer (10x) | Cell signaling Technology |
| Chloroform | AppliChem |
| Clarity ECL Western Blotting Substrate | Bio-Rad |
| DPBS | Gibco |
| Ethanol | Sigma Aldrich |
| Ethanol absolute, molecular biology grade | AppliChem |
| Ethylenediaminetetraacetic acid (EDTA) | Thermo Fisher Scientific |
| Glycine | Roth |
| Isopropyl alcohol | Sigma Aldrich |
| Methanol | Sigma Aldrich |
| Milk powder | Roth |

| | |
|---|---|
| N,N,N',N'-Tetramethylethylenediamine (TEMED) | Roth |
| PageRuler Prestained Protein Ladder | Thermo Fisher Scientific |
| Phosphate buffered saline (PBS) | Gibco |
| Tween 20 | Sigma Aldrich |
| Ponceau S | Sigma Aldrich |
| QIAzol Lysis Reagent | Qiagen |
| RNase-free water | Merck Millipore |
| RNase Zap | Thermo Fisher Scientific |
| Sodium dodecyl sulfate (SDS) | Roth |
| Spectra Multicolor High Range Protein Ladder | Roth |
| TaqMan® Universal PCR Master Mix | Applied Biosystems |
| Trizma® base | Roth |

## 3.3  Consumable materials

| | |
|---|---|
| 384-well plate | Sarstaedt |
| 96-well plate | Sarstaedt |
| Blotting paper (Whatman 3MM) | Schleicher & Schuell |
| Cryo tubes (1.5, 2 ml) | Thermo Fisher Scientific |
| Distilled water | Gibco |
| Falcon tubes (5, 15, 50 ml) | Corning Inc. |
| Filter paper | Roth |
| Gloves | Ansell |
| Micro tubes (0.5, 1.5, 2 ml) | Eppendorf AG |
| Mouse GeneChip 1.0 ST Array | Affymetrix |
| Multiply MStrip 8er-strip | Sarstaedt |
| Multiply PCR plate | Sarstaedt |
| Nitrocellulose membrane | Bio-Rad |
| Nunc 96-well plate | Thermo Fisher Scientific |
| Optical PCR plate (96-well and 384-well) | Thermo Fisher Scientific |
| Optical adhesive cover | Applied Biosystems |
| Pipette tips (for 2, 10, 100, 1000 µl pipettes) | Sarstaedt |
| Pipette tips (1-10 µl) | Rainin |
| Pipette filter tips (for 2, 10, 100, 1000 µl pipettes) | Biosphere |

| | |
|---|---|
| RNA 6000 Nano Chip | Agilent |
| Small RNA Chip | Agilent |

## 3.4  Kits

| | |
|---|---|
| Ambion WT Expression Kit | Ambion |
| GeneChip® Hybridization, Wash and Stain Kit | Affymetrix |
| GeneChip® WT Terminal Labeling and Hybridization Kit | Affymetrix |
| High-Capacity cDNA Reverse Transcription Kit | Thermo Fisher Scientific |
| Pierce BCA Protein Assay Kit | Thermo Fisher Scientific |
| RNA 6000 Nano Kit | Thermo Fisher Scientific |
| Small RNA Kit | Thermo Fisher Scientific |
| TaqMan® Gene Expression Assay | Thermo Fisher Scientific |
| TaqMan® MicroRNA Reverse Transcription Kit | Thermo Fisher Scientific |
| TaqMan® Small RNA Assay | Thermo Fisher Scientific |
| TruSeq Small RNA Library Preparation Kit | Illumina |

## 3.5  Laboratory equipment

| | |
|---|---|
| 2100 Agilent Bioanalyzer | Agilent |
| 7900HT Fast Real-Time PCR System | Thermo Fisher Scientific |
| Analytical balance (AG245) | Mettler Toledo |
| Bandelin sonication system | Bandelin electronic |
| Blotting system | Bio-Rad |
| Centrifuge 5810 and 5804R | Eppendorf |
| Electrophoresis system Mini-PROTEAN® | Bio-Rad |
| GeneChip® AutoLoader | Affymetrix |
| GeneChip® Fluidics Station 450 | Affymetrix |
| GeneChip® Hybridization Oven 640 | Affymetrix |
| GeneChip® Scanner 3000 7G | Affymetrix |
| Heraeus Megafuge 16R | Thermo Fisher Scientific |
| Haraeus Fresco 21 Centrifuge | Thermo Fisher Scientific |
| HiSeq 2500 System | Ilumina |

| | |
|---|---|
| Microplate Reader (Tecan Infinite M200) | Tecan |
| Microwave | Sharp |
| Multichannel pipette 1-10 µl | Rainin |
| PCR cycler (GeneAmp® PCR System 9700) | Applied Biosystems |
| pH-meter CG840 | Schott |
| Pellet pestle | Sigma Aldrich |
| Pipetboy | Integra Bioscience |
| Pipettes Eppendorf Research (2,10,100,1000 µl) | Eppendorf |
| Spectrophotometer (NanoDrop ND-2000c) | Thermo Fisher Scientific |
| Table centrifuge | Fisherbrand |
| Thermomixer 5436 | Eppendorf |
| Thermoshaker | Labotec |
| Thermoscientific Matrix Pipette | Thermo Fisher Scientific |
| Vortexer (Vortexgenie 2) | Scientific industries |

## 3.6 Gene and miRNA expression assays

All used TaqMan® assays (Thermo Fisher Scientific) for gene and miRNA expression analysis are shown in Table 1 and Table 2.

**Table 1: Gene expression assays for quantitative real-time PCR**

| Gene | Gene name | Assay ID |
|---|---|---|
| 18S rRNA | 18S ribosomal RNA | Hs99999901_s1 |
| *B4galt6* | beta-1,4-galactosyltransferase 6 | Mm00480045_m1 |
| *Ccbe1* | collagen and calcium binding EGF domains 1 | Mm00618932_m1 |
| *Ccl11* | chemokine (C-C motif) ligand 11 | Mm00441238_m1 |
| *Cdkn1a* | cyclin-dependent kinase inhibitor 1A (P21) | Mm04205640_g1 |
| *Ctgf* | connective tissue growth factor | Mm00515790_g1 |
| *Gatm* | glycine amidinotransferase | Mm01268678_m1 |
| *Hcn2* | hyperpolarization-activated cyclic nucleotide-gated ion channel 2 | Mm00468538_m1 |
| *Hcn4* | hyperpolarization-activated cyclic nucleotide-gated ion channel 4 | Mm01176086_m1 |
| *Nppa* | natriuretic peptide type A | Mm01255748_g1 |
| *Pip5k1b* | phosphatidylinositol-4-phosphate 5-kinase, type 1 beta | Mm00476828_m1 |
| *Scn4a* | sodium channel, type IV, alpha | Mm00500103_m1 |
| *Scn4b* | sodium channel, type IV, beta | Mm01175562_m1 |
| *Ucp2* | uncoupling protein 2 | Mm00627599_m1 |

ID: identification; PCR: polymerase chain reaction.

**Table 2: miRNA expression assays for quantitative real-time PCR**

| miRBase ID | Assay name | Assay ID |
|---|---|---|
| mmu-let-7i-5p | hsa-let-7i | 002221 |
| mmu-miR-30b-5p | hsa-miR-30b | 000602 |
| mmu-miR-30d-3p | hsa-miR-30d | 000420 |
| mmu-miR-100-5p | hsa-miR-100 | 000437 |
| mmu-miR-125b-5p | hsa-miR-125b | 000449 |
| mmu-miR-130a-3p | hsa-miR-130a | 000454 |
| mmu-miR-181c-5p | hsa-miR-181c | 000482 |
| mmu-miR-192-5p | hsa-miR-192 | 000491 |
| mmu-miR-204-5p | hsa-miR-204 | 000508 |
| mmu-miR-210-3p | hsa-miR-210 | 000512 |
| snoRNA202 | snoRNA202 | 001232 |

ID: identification; PCR: polymerase chain reaction.

# 4 Methods

## 4.1 Animal model

### 4.1.1 AGAT knockout mouse model

Choe et al. developed an AGAT-deficient knockout (AGAT$^{-/-}$) mouse model. In brief, using C57BL/6J mice, exon 3 of the AGAT gene was disrupted by insertion of a selection cassette containing the neomycin resistance gene (Neo) flanked by Lox-P sites (Figure 3 A). As a result, AGAT$^{-/-}$ mice express a shortened instable mRNA that cannot be translated into a protein (Figure 3 B).
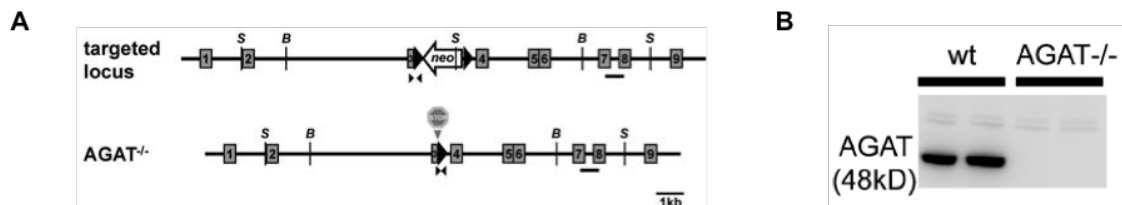


**Figure 3: AGAT knockout mouse model**
**A**, Generation of AGAT knockout (AGAT$^{-/-}$) mice by disruption of exon 3. **B**, AGAT protein expression in wild-type (wt) compared to AGAT$^{-/-}$ mice. Figure from Choe et al., 2013b, Figure 1 A and C: Generation of AGAT mice.

The respective local animal ethics committees approved all experimental procedures and investigations applied to the animal model were conformed to the guidelines for the care and use of laboratory animals published by the NIH (Publication No. 85-23, revised 1996). Mice were obtained from heterozygous breeding after backcrossing to a C57BL/6J genetic background for at least six generations. All analyzed animals were littermates. The mice (< 5 per cage) were kept in standard cages under a 12 h:12 h light:dark cycle, constant temperature and humidity and received standard food and water *ad libitum*. In the following study, the effects of the AGAT knockout as well as the effects of a supplementation with homoarginine or creatine were investigated. Therefore, four groups of mice were defined: Wild-type (WT) mice, AGAT$^{-/-}$ mice and AGAT$^{-/-}$ mice supplemented either with homoarginine (AGAT$^{-/-}$HA) or creatine (AGAT$^{-/-}$Cr). The 4-week-long supplementation with homoarginine was achieved

via osmotic mini pumps. Creatine supplementation was achieved by addition of 1% creatine to chow (Ssniff) from birth on.

### 4.1.2 *In vivo* model of myocardial infarction

Experimental induced MI in C57BL/6J WT mice was performed by AG Westermann (Clinic for General and Interventional Cardiology, University Heart Centre Hamburg). MI was conducted by permanent ligation of the left descending coronary artery as described previously (Riad et al., 2008). Sham-operated mice undergoing the same surgical procedure without ligation of the coronary artery served as controls. Five days after MI, samples of the infarcted and the non-infarcted area of the left ventricle were collected.

### 4.1.3 Organ extraction and tissue preparation

Mice in the AGAT knockout study were anesthetized with 2-3% isoflurane in 100% oxygen. After median thoracotomy, aorta, brain, heart, liver and kidneys were extracted. The left ventricle of the heart was prepared and all tissues were shock frozen in liquid nitrogen for storage at -80 °C. Prior to use, frozen tissue was powdered with a steel mortar and pestle in liquid nitrogen and split for separated preparation of mRNA, miRNA and proteins.

## 4.2 RNA analysis

### 4.2.1 Total RNA isolation

QIAzol lysis reagent was used for the isolation of total RNA from mice. QIAzol (similar to TRIzol) is a monophasic solution of phenol and guanidine thiocyanate that allows the disruption of cells and tissues while protecting RNA from degradation through RNases (Chomczynski and Sacchi, 1987). 500 µl of QIAzol per 10-20 µg of tissue powder was used for the homogenization with a pellet pestle. The homogenate was incubated at room temperature for 5 min and 100 µl chloroform was added. After shaking the tube for 15 seconds per hand, the samples were centrifuged (12,000 g; 15 min; 4 °C). The mixture separates into a lower red phenol-chloroform phase, an interphase and a colorless upper aqueous phase. The upper phase contains the RNA and was transferred into a new

nuclease-free 1.5 ml tube. 250 µl of isopropanol was used to precipitate the RNA for 10 min at room temperature. After centrifugation (12,000 g; 10 min; 4 °C) the RNA forms a gel-like pellet on the side and bottom of the tube. The supernatant was discarded and the pellet was washed with 500 µl 80% ethanol and centrifuged again (7,500 g; 5 min; 4 °C). The washing step was performed twice. After washing, the pellet was allowed to dry for 10 min at room temperature and dissolved in an appropriate amount of nuclease-free water (30-50 µl). RNA was stored at -80 °C until utilization.

### 4.2.2  RNA quantity and quality control

**Determination of the RNA concentration**

RNA concentration and purity were determined using the NanoDrop Spectrophotometer by measuring the absorbance at a wavelength of 260 nm. It was assumed that 1 unit of absorbance corresponds to 40 µg/ml. Absorbance was also determined at the wavelength of 280 nm and the ratio A260/A280 was calculated to evaluate RNA purity.

**Determination of the RNA integrity**

RNA quality is of critical importance when considering the success of downstream molecular applications. As a standardized tool to assess the quality of the RNA, the RNA integrity number (RIN) was determined. The RIN allows the classification of total RNA, based on a numbering system from 1 to 10, with 1 being the most degraded profile and 10 being the most intact (Schroeder et al., 2006). The Agilent 2100 Bioanalyzer and associated RNA 6000 Nano Chip were used for this approach. Total RNA was prepared according to the instructions of the RNA 6000 Nano Kit and the 2010 Expert Software conducted the data evaluation. Figure 4 shows an example of result representation via gel-like image and electropherogram.
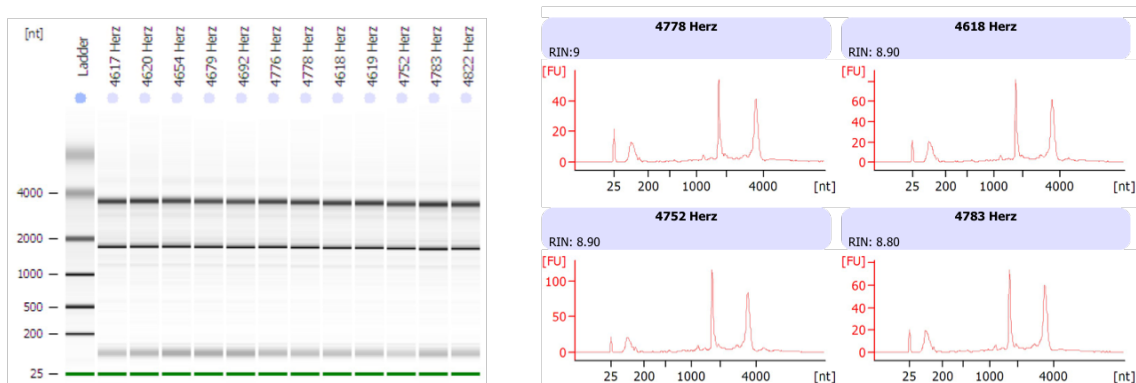
**Figure 4: Determination of the RNA integrity**
For analysis the Agilent 2100 Bioanalyzer was used. Representative gel-like image (left) and electropherograms (right) of heart tissue samples are shown. A RNA integrity number (RIN) of 8.8-9 indicates a good quality of total RNA with almost no degradation.

## Determination of miRNA content in total RNA

To evaluate the miRNA content in total RNA samples the Agilent Small RNA Chip was used with the Agilent 2100 Bioanalyzer. The chip allows comparing small RNA regions and analyze miRNA yields. It is critical that total RNA samples are initially evaluated for integrity, since the degradation of total RNA leads to the accumulation of small RNA fragments resulting in an overestimation of the miRNA and small RNA content. The RIN should be > 8 to get reliable results with the Small RNA Chip. Total RNA samples were prepared according to the instructions of the Agilent Small RNA Kit. Data analysis was carried out using the 2100 Expert Software. For further downstream applications the RNA samples should contain more than 0.5% small RNA in the ~ 10–40 nt size range.

### 4.2.3   Reverse transcription

#### Reverse transcription of total RNA

The cDNA synthesis was performed using the High-Capacity cDNA Reverse Transcription Kit (Thermo Fisher Scientific). In brief, a 2-fold reverse transcription master mix (Table 3) was prepared and added to the equal volume of RNA template. Therefore, 1 µg RNA isolated from mouse tissue was diluted in nuclease-free water to a final volume of 10 µl and denatured for 10 min at 70 °C. Subsequently, the master mix was added and reverse transcription was performed in a thermal cycler (Table 4). After polymerase chain reaction (PCR),

180 µl nuclease-free water was added to 20 µl reaction product and stored at -20 °C.

**Table 3: Master mix composition for cDNA synthesis**

|  | Original Concentration | Concentration (Master mix) | Vol. [µl] |
|---|---|---|---|
| RNA Template | 100 ng/µl | 50 ng/µl | 10 |
| Random Primer | 10x | 1x | 2 |
| dNTP Mix | 25x dNTP mix (100 mM) | 1x | 0.8 |
| RT Buffer | 10x | 1x | 2 |
| Nuclease-free Water | - | - | 4.2 |
| Multiscribe RT | 50 U/µl | 2.5 U/µl | 1 |
| **Total Volume** |  |  | **20 µl** |

cDNA: complementary deoxyribonucleic acid; dNTP: deoxynucleoside triphosphate; RNA: ribonucleic acid; RT: reverse transcriptase; Vol.: volume.

**Table 4: Cycler program for cDNA synthesis**

| Temperature [°C] | Time [min] | Step |
|---|---|---|
| 25 | 10 | Primer Annealing |
| 37 | 120 | Reverse Transcription |
| 85 | 5 | Inactivation of Reverse Transcriptase |
| 4 | ∞ | Cooling |

cDNA: complementary deoxyribonucleic acid.

## Reverse transcription of miRNAs

The TaqMan® MicroRNA Reverse Transcription Kit (Thermo Fisher Scientific) was used for the cDNA synthesis of miRNAs. To produce a template that can be analyzed in standard TaqMan® Assay-based real-time PCR, the Kit is used with a target-specific stem-loop primer to extend the 3' end of the mature miRNA. This design allows the construction of a specific cDNA for every miRNA. All primers are included in the TaqMan® Small RNA Assay and listed in 3.6, Table 2. For medium-scale orders, the reverse transcriptase (RT) primer is supplied in 20x concentration that must be diluted to a 5x working stock dilution in 0.1x TE buffer. The preparation was then carried out in three steps. First a 10 µl master mix of dNTPs, RT, RT buffer, RNase inhibitor and nuclease-free water was prepared. Subsequently, the diluted total RNA (5 ng/µl) and the RT primer were added. The final concentration of all components is shown in Table 5. The PCR was performed in a thermal cycler (Table 6). The 15 µl reaction product was stored at -20 °C until utilization.

**Table 5: Master mix composition for cDNA synthesis of miRNAs**

|  | Original Concentration | Concentration (Master mix) | Vol. [µl] |
|---|---|---|---|
| RNA Template | 5 ng/µl | 0.67 ng/µl | 2 |
| RT Primer | 5x | 1x | 3 |
| dNTP Mix | 25x dNTP mix (100 mM) | 0.25x | 0.15 |
| RT Buffer | 10x | 1x | 1.5 |
| Nuclease-free Water | - | - | 7.16 |
| Multiscribe RT | 50 U/µl | 3.3 U/µl | 1 |
| RNase Inhibitor | 20 U/µl | 0.25 U/µl | 0.19 |
| **Total Volume** |  |  | **15 µl** |

cDNA: complementary deoxyribonucleic acid; dNTP: deoxynucleoside triphosphate; RNA: ribonucleic acid; RT: reverse transcriptase; Vol.: volume.

**Table 6: Cycler program for cDNA synthesis of miRNAs**

| Temperature [°C] | Time [min] | Step |
|---|---|---|
| 16 | 30 | 1 |
| 42 | 30 | 2 |
| 85 | 5 | 3 |
| 4 | ∞ | Cooling |

cDNA: complementary deoxyribonucleic acid; miRNA: micro ribonucleic acid.

## 4.2.4  Quantitative polymerase chain reaction

The expression levels of mRNAs and miRNAs were determined by quantitative real-time polymerase chain reaction (qPCR) using cDNA-based probes (TaqMan® probes, Thermo Fisher Scientific). This method enables the detection of accumulated PCR amplicons through an increase in the fluorescence intensity. The quantitative analysis was performed with the TaqMan® 7900HT Fast Real-Time PCR System (Thermo Fisher Scientific). The relative mRNA or miRNA concentrations are determined during the exponential phase of the qPCR amplification by plotting the fluorescence signal against the cycle number on a logarithmic scale. The point at the beginning of the exponential phase in which the fluorescence signal exceeds the background signal is set as the Cycle threshold (Ct).

### mRNA expression analysis

For mRNA expression analysis, the TaqMan® Gene Expression Assay (Thermo Fisher Scientific; 3.6, Table 1) was used. cDNA from the AGAT^{-/-} mouse model was prepared as described in 4.2.3 and used in a concentration of 5 ng/µl. cDNA from mice after MI was kindly provided by AG Westermann. The cDNA had a

concentration of 10 ng/µl and 2 µl per sample were available. Since the expression of many genes had to be determined, a dilution of 1:10 was carried out. Accordingly, the final concentration of the MI cDNA templates was 1 ng/µl. The components for the qPCR reaction and the cycling parameters are shown below (Table 7, Table 8).

**Table 7: qPCR reaction for mRNA expression analysis**

| Component | Vol. [µl] |
|---|---|
| 20x TaqMan® Gene Expression Assay | 0.5 |
| 2x TaqMan® Gene Expression Master Mix | 5 |
| cDNA Template | 2 |
| Nuclease-free Water | 2.5 |
| **Total Volume** | **10 µl** |

cDNA: complementary deoxyribonucleic acid; qPCR: quantitative real-time polymerase chain reaction; Vol.: volume; mRNA: messenger ribonucleic acid.

**Table 8: qPCR cycler program for mRNA expression analysis**

| Temperature [°C] | Time [min] | Step | Repetitions |
|---|---|---|---|
| 50 | 2 | Uracil-N-Glycosylase Activation | 1x |
| 95 | 10 | Initial Denaturation + Uracil-N-Glycosylase Inactivation | 1x |
| 95 | 0.25 | Denaturation | 40x |
| 60 | 1 | Annealing and Elongation | |

qPCR: quantitative real-time polymerase chain reaction; mRNA: messenger ribonucleic acid.

**miRNA expression analysis**

The TaqMan® Small RNA Assay was carried out to quantify miRNA expression. The Assay Kit includes the specific primer for cDNA synthesis as well as the TaqMan® probe for qPCR (3.6, Table 2). cDNA synthesis was performed as described in 4.2.3. The qPCR reaction for miRNA expression analysis and the cycling parameters are shown below (Table 9, Table 10). Each sample was analyzed in triplicates and normalized to an endogenous control (snoRNA202).

**Table 9: qPCR reaction for miRNA expression analysis**

| Component | Vol. [µl] |
|---|---|
| 20x TaqMan® Small RNA Assay | 1 |
| 2x TaqMan® Gene Expression Master Mix | 10 |
| cDNA Template | 1.33 |
| Nuclease-free Water | 7.67 |
| **Total Volume** | **20 µl** |

cDNA: complementary deoxyribonucleic acid; qPCR: quantitative real-time polymerase chain reaction; Vol.: volume; miRNA: micro ribonucleic acid.

**Table 10: qPCR cycler program for miRNA expression analysis**

| Temperature [°C] | Time [min] | Step | Repetitions |
|---|---|---|---|
| 50 | 2 | Uracil-N-Glycosylase Activation | 1x |
| 95 | 10 | Initial Denaturation + Uracil-N-Glycosylase Inactivation | 1x |
| 95 | 0.25 | Denaturation | }40x |
| 60 | 1 | Annealing and Elongation | |

qPCR: quantitative real-time polymerase chain reaction; miRNA: micro ribonucleic acid.

### 4.2.5 Microarray

**mRNA expression analysis**

In order to analyze the expression level of large numbers of genes simultaneously, microarray experiments were performed using the Affymetrix Mouse GeneChip 1.0 ST Array. This method allows determining the expression of genes by measuring the presence of the corresponding mRNA transcripts in a sample. On an Array-Chip, every gene is represented by several single-stranded oligonucleotide sequences (probes), which are bound to the chip surface. The hybridization of processed, fluorescent-labeled mRNA targets to the probes can then be
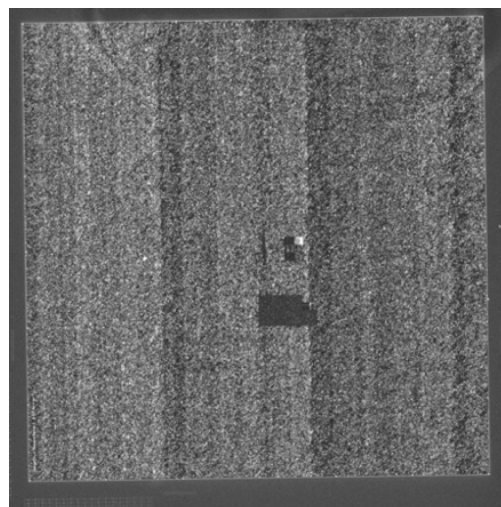


**Figure 5: Example of a scanned Affymetrix Mouse GeneChip 1.0 ST Array**

Every bright spot represents a detected gene. The stronger the signal, the more transcripts of this gene are present in the hybridized sample. The dark square is an area for hybridization control set by Affymetrix.

detected by laser scanning (Figure 5). Total strength of the laser signal depends upon the amount of mRNA target binding to the probe. The preparation of left ventricular heart tissue samples was conducted using the Ambion WT Expression Kit and the Affymetrix GeneChip WT Terminal Labeling and Hybridization Kit. All steps of preparation were performed according to manufacturer's recommendations. Briefly, 250 ng of high quality total RNA (RIN > 8) were reverse-transcribed using primers containing a T7 promoter sequence for the first-strand cDNA synthesis reaction. After DNA polymerase- and RNase H-mediated second-strand cDNA synthesis, the double-stranded cDNA was purified and served as a template for the *in vitro* transcription reaction which

generates antisense complementary RNA (cRNA). The cRNA was cleaned up and a sense-strand cDNA was synthesized. Prior to the hybridization to the microarrays (16 h, 45 °C), the sense-strand cDNA was fragmented and labeled with biotin. The GeneChips were then washed and stained on an Affymetrix Fluidics Station 450 and scanned on an Affymetrix GeneChip 3000 scanner. All samples were processed simultaneously, including one control RNA sample provided by Affymetrix.

### 4.2.6  miRNA sequencing

Next-generation sequencing was carried out to study miRNA expression profiles. The miRNA library preparation as well as the miRNA sequencing was performed at the Max Delbrück Centre for Molecular Medicine (MDC) in Berlin (Prof. Dr. Norbert Hübner). Prior to the processing of the samples in Berlin, the RIN and the amount of miRNAs in total RNA was evaluated using the 2100 Agilent Bioanalyzer (4.2.2). Only samples with a RIN > 8 were used for further analysis. Small RNA sequencing libraries were created following the TruSeq Small RNA Library Preparation Kit protocol. In brief, 3' and 5' RNA adapter, specifically modified to target the ends of miRNA molecules, were ligated to 1 μg of high quality total RNA. Reverse transcription was used to generate single-stranded cDNA libraries and PCR was performed to amplify and add unique index sequences to each library. The addition of index sequences makes it possible to distinguish different samples from each other and therefore analyze several samples simultaneously. The sequencing was carried out with the Illumina HiSeq 2500 System, which uses the sequencing by synthesis technology (Illumina, 2010). For each sample the number of different miRNA reads was generated and analyzed with bioinformatics techniques as described in 4.5.1.

## 4.3  Protein analysis

### 4.3.1  Protein extraction from tissue

For protein extraction about 20-30 mg tissue powder was mixed up with 200-300 μl cell lysis buffer (Cell signaling Technology). The tissue was homogenized using a pellet pestle and vortexed briefly. All samples were

prepared simultaneously and kept on ice after homogenization. Subsequently, the homogenate was sonicated three times for 15 seconds and incubated on a thermomixer (800 rpm; 10 min; 4 °C). After centrifugation (max speed; 30 min; 4 °C), the supernatant was collected and stored at -20 °C prior to use for western blot.

### 4.3.2 Determination of protein concentration

Concentration of proteins was determined using the bicinchoninic acid (BCA) assay (Smith et al., 1985). The principle of this method is the reduction of $Cu^{+2}$ to $Cu^{+1}$ in an alkaline solution (the biuret reaction) combined with the colorimetric detection of the cuprous cation ($Cu^{+1}$) using a reagent containing BCA. The purple-colored reaction product is formed by the chelation of two molecules of BCA with one cuprous ion. This complex exhibits a strong absorbance at 562 nm that is nearly linear with increasing protein concentrations. The samples were prepared according to manufacturer's instructions (Pierce BCA Protein Assay Kit). In brief, 25 µl of protein samples or standards of bovine serum albumin (BSA; 20-2000 µg/ml) and 200 µl working solution were mixed in a microplate well. After incubation at 37 °C for 30 min, the absorbance was measured on the Tecan Microplate Reader. Samples were measured in duplicates. The protein quantity was determined based on a standard curve prepared by plotting the average 562 nm measurements for each BSA standard versus its concentration in µg/ml.

### 4.3.3 Western blot analysis

Total protein lysates from tissue powder (40 µg) were separated by sodium dodecyl sulfate polyacrylamide gel electrophoresis (SDS-PAGE). Prior separation, protein samples were mixed (1:3) with 4x Laemmli buffer containing 4% ß-mercaptoethanol and denatured for 5 min at 95 °C. The polyacrylamide gel consisted of a stacking gel (125 mM Tris base, pH 6.8; 5% acrylamide/bis acrylamide solution (29:1); 0.1% SDS; 0.1% APS; 0.08% TEMED) and a running gel (375 mM Tris base, pH 8.8; 12% acrylamide/bis acrylamide solution (29:1); 0.1% SDS; 0.1% APS; 0.03% TEMED) that separates the proteins according to the molecular size. After preparation, the gel was placed into the electrophoresis chamber filled with 1x SDS-running buffer (25 mM Tris base; 192 mM glycine;

0.1% SDS). As a molecular weight marker the PageRuler™ Prestained Protein Ladder was used. Electrophoresis was performed at 130 V until the bromophenol blue in the loading buffer ran out of the gel (for most proteins ~ 60-90 min). Following electrophoresis, proteins were transferred on nitrocellulose (NC) membranes by wet-electroblotting at 100 mA per gel for 90 min at 4 °C in a blotting chamber system using transfer buffer (50 mM Tris base; 380 mM glycine; 0.1% SDS; 20% ethanol). Subsequently, the NC membrane was stained with Ponceau S and washed three times with 1x TBS-T (100 mM Tris base, pH 7.5; 150 mM NaCl; 0.1% Tween 20). To block remaining hydrophobic binding sites and avoid unspecific bindings, the membranes were incubated in 5% milk in 1x TBS-T powder solution or 5% BSA in 1x TBS-T solution for two times 30 min at room temperature. Membranes were stained overnight with primary antibodies (Table 11) diluted in 5% milk powder/BSA in 1x TBS-T at 4 °C under gentle agitation. The membrane was washed three times with 1x TBS-T and incubated with the corresponding secondary antibody (Table 11) diluted in 5% milk powder/BSA in 1x TBS-T solution for 1 h at room temperature. After three more washing steps in 1x TBS-T proteins were visualized using the Clarity™ ECL Western Blotting Substrate (Bio-Rad) according to the manufacturer's instructions. The produced chemiluminescent signal was detected at different time points with the Fusion Solo S system (Vilber Lourmat) and analyzed using the Vision-Capt Software.

**Table 11: Antibodies used for western blot analysis**
The primary and secondary antibodies (AB) have been diluted in either 5% milk powder in 1x TBS-T (CDKN1A, CTGF, UCP2) or 5% BSA in 1x TBS-T (GAPDH).

| Protein | Primary AB | Dilution | Secondary AB | Dilution |
|---------|-----------|----------|--------------|----------|
| CDKN1A | Anti-p21/WAF1/Cip1, monoclonal | 1:1000 | Anti-mouse IgG | 1:10000 |
| CTGF | Anti-CTGF, polyclonal | 1:2000 | Anti-rabbit IgG | 1:10000 |
| GAPDH | GAPDH (14C10), monoclonal | 1:5000 | Anti-rabbit IgG | 1:10000 |
| UCP2 | Anti-UCP2, polyclonal | 1:500 | Anti-rabbit IgG | 1:10000 |

## 4.4  Bioinformatics databases and tools

### 4.4.1  GEO

GEO (Gene Expression Omnibus) (ncbi.nlm.nih.gov/geo/) is a public database containing data from several high-throughput genomic approaches such as microarrays and next-generation sequencing. The data are submitted by the scientific community (Edgar et al., 2002). To query and download the studies and gene expression patterns, several web-based interfaces and applications are available online. Additionally, gene expression analysis can be performed using the GEO2R program. In this study, the microarray experiment with the GEO accession number GSE775 (Mouse model of myocardial infarction) was used.

### 4.4.2  WebGestalt

WebGestalt (WEB-based GEne SeT AnaLysis Toolkit) (www.webgestalt.org/) is a publicly available analysis toolkit for functional genomic, proteomic and large-scale genetic studies from which large number of gene lists are continuously generated (Zhang et al., 2005). Pathway analyses (Wikipathways) of differentially expressed gene sets were performed in order to identify an enrichment of genes in metabolic or disease-related pathways. The gene sets are adjusted for multiple testing based on the Benjamini-Hochberg method (Benjamini & Hochberg 1995) and a significance level of ≤ 0.05 was set for statistical significance.

### 4.4.3  miRDB

In order to identify mRNA-miRNA interactions, the online database miRDB (www.mirdb.org/miRDB) for miRNA target prediction and functional annotations was used. All the targets in miRDB were predicted by a bioinformatics tool, MirTarget, which was developed by analyzing thousands of miRNA-target interactions from high-throughput sequencing experiments (Wong and Wang, 2015). The database allows the user either to search by miRNA name or by gene target. After analysis, every predicted target gets a target prediction score between 50-100. The higher the score, the more confidence in this prediction is given. miRNA-mRNA interactions with a target prediction score > 80 were assumed to be real and used for further investigations.

## 4.5  Statistical and bioinformatics analysis

### 4.5.1  Analysis of gene and miRNA expression

**Analysis of expression levels measured by qPCR**

The mRNA and miRNA levels were quantified according to the $2^{-\Delta\Delta Ct}$ method by Livak and Schmittgen (Livak and Schmittgen, 2001). For comparison of two groups (not normally distributed), the nonparametric Mann-Whitney-Test was used. For comparison of multiple groups, the nonparametric Kruskal-Wallis-Test was used. Differences were considered statistically significant at a value of $P \leq 0.05$. All calculations were performed using Graph Pad Prism 7. qPCR was also used to validate the AGAT knockout and to check the correct matching of the mice to the different groups.

**Analysis of expression levels measured by microarray**

Microarray analyses of murine gene expression were performed using the statistical language R (Team, 2008). R/Bioconductor (www.bioconductor.org) package *xps* was used for pre-processing of the microarrays. In order to retrieve comparable metrics of gene expression between chips, the *xps* function *rma* was used for background correction and normalization. For each gene, the probability of being expressed was calculated and only genes expressed in at least two samples per group were kept for further analysis. Overall differences in gene expression between groups of mice were assessed by principal component analysis (PCA). This method helps to separate the overall variance into independent components, each explained by different technical or biological factors. The first two principal components were plotted against each other to visualize potential clustering of samples into groups representing treatment conditions. Differential gene expression was calculated between groups using R/Bioconductor package *limma*. To account for multiple testing, the false discovery rate (FDR) based Benjamini-Hochberg method (Benjamini and Hochberg 1995) was used. Differentially expressed genes with a FDR $\leq 0.05$ were considered significant.

**Analysis of expression levels measured by miRNA sequencing**

The CLC Genomics Workbench (clcbio.com/products/clc-genomics-workbench/) was used to map reads from miRNA sequencing against the murine set of all known miRNAs, which was retrieved from miRBase (www.mirbase.org/). The number of reads falling in mature miRNAs were extracted and further processed in R. Differential expression of miRNAs between groups of mice was calculated by R/Bioconductor package *DESeq* (Anders and Huber, 2010). Only miRNAs covered by more than ten reads were kept for further analyses. Differentially expressed miRNAs with a FDR ≤ 0.05 were considered significant.

### 4.5.2  Network analysis of gene expression

Weighted correlation network analysis (WGCNA) was used for the identification of clusters (modules) of highly correlated genes (Langfelder and Horvath, 2008). For each module, the so-called eigengene was calculated, which represents the first principal component after performing a PCA using all genes in the module. Associations between eigengenes of each module and sample origin (WT and AGAT$^{-/-}$) were calculated to identify modules highly deregulated in AGAT$^{-/-}$ mice. Subsequently, literature-based research was carried out in order to identify genes in the two top networks (selection criterion: smallest P-value) with an association to the cardiovascular system. These genes were further classified as candidate genes.

### 4.5.3  Analysis of protein expression

The calculated volume of every protein was normalized to an endogenous control (GAPDH). Data were plotted using GraphPad Prism 7 and shown as mean and standard error of the mean (SEM). For comparison of two groups (not normally distributed), the nonparametric Mann-Whitney-Test was used. For comparison of more than two groups, the nonparametric Kruskal-Wallis-Test was performed.

# 5 Results

The goal of the present study was to investigate the molecular mechanisms and pathways involved in the AGAT and homoarginine/creatine metabolism, since different homoarginine plasma levels and genetic variants within the *AGAT* gene were found to predict cardiovascular mortality (März et al., 2010, Pilz et al., 2011b, Atzler et al., 2014, Choe et al., 2013a). Moreover, AGAT$^{-/-}$ mice exhibit cardiac dysfunction, which was corrected in part by creatine and completely by supplementation of homoarginine (Faller et al., 2017). Therefore, in the following thesis, heart tissue samples of an AGAT$^{-/-}$ mouse model were used to gain molecular insights on mRNA and miRNA level. In order to study the clinical impact, the findings were finally translated into a disease model of MI.

## 5.1 Analysis of AGAT-related gene expression in the heart

In order to evaluate the effects of the AGAT knockout and homoarginine/creatine on transcriptome level, microarray experiments in murine left ventricular heart tissues were performed. The analysis of gene expression was conducted in four groups of mice: Wild-type (WT; n = 7), AGAT knockout (AGAT$^{-/-}$; n = 7) and AGAT knockout mice supplemented with homoarginine (AGAT$^{-/-}$HA; n = 5) or creatine (AGAT$^{-/-}$Cr; n = 4).

### 5.1.1 Validation of the AGAT knockout by qPCR

To confirm the AGAT knockout in murine heart tissue samples, total RNA was isolated, reverse transcribed into cDNA and used as a template for qPCR amplification. The *Agat* mRNA transcript consists of 9 exons and the knockout leads to a stop of the transcription at exon 3. Since the binding site of the used TaqMan® probe spans from exon 3 to exon 4, *Agat* mRNA should not be or should be less amplified in AGAT$^{-/-}$ mice. Figure 6 shows the mRNA expression in WT, AGAT$^{-/-}$, AGAT$^{-/-}$HA and AGAT$^{-/-}$Cr littermates. The mRNA level was markedly lower in the AGAT$^{-/-}$ compared to the WT group. Until a Ct value of 38, no

amplification was observed in AGAT$^{-/-}$ mice, whereas the WT showed a Ct value at around 30.
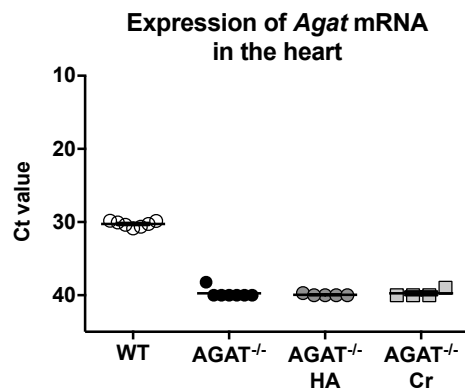


**Figure 6: Validation of the AGAT knockout by qPCR**
*Agat* mRNA expression in murine heart tissue of wild-type (WT; n = 7), AGAT knockout (AGAT$^{-/-}$; n = 7), homoarginine-supplemented AGAT knockout (AGAT$^{-/-}$HA; n = 5) and creatine-supplemented AGAT knockout (AGAT$^{-/-}$Cr; n = 4) mice was compared to each other. A Ct value specified as undetermined was set to 40 cycles. Ct: Cycle threshold.

### 5.1.2 Principle component analysis

As a first tool to assess overall gene expression between groups of mice, a PCA was performed. The first two principal components were plotted against each other to visualize potential clustering of samples into groups. Each dot represents one sample and each color one of the four mouse groups respectively. Based on this plot, two clusters of samples were identified: WT (green) and AGAT$^{-/-}$Cr (black) as well as AGAT$^{-/-}$ (red) and AGAT$^{-/-}$HA (blue) (Figure 7).
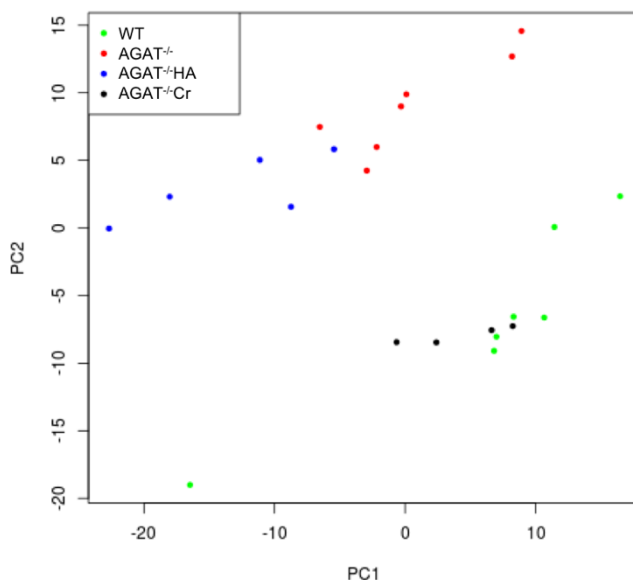


**Figure 7: Principle component analysis of murine heart tissue samples**
The first two principle components (PC1 and PC2) of wild-type (WT; n = 7), AGAT knockout (AGAT$^{-/-}$; n = 7), homoarginine-supplemented AGAT knockout (AGAT$^{-/-}$HA; n = 5) and creatine-supplemented AGAT knockout (AGAT$^{-/-}$Cr; n = 4) mice were plotted against each other.

## 5.1.3 Differential gene expression in AGAT knockout mice

The number of differentially expressed genes between the groups was evaluated for each comparison as shown in Figure 8. After correction for multiple testing, the FDR was set to ≤ 0.05.
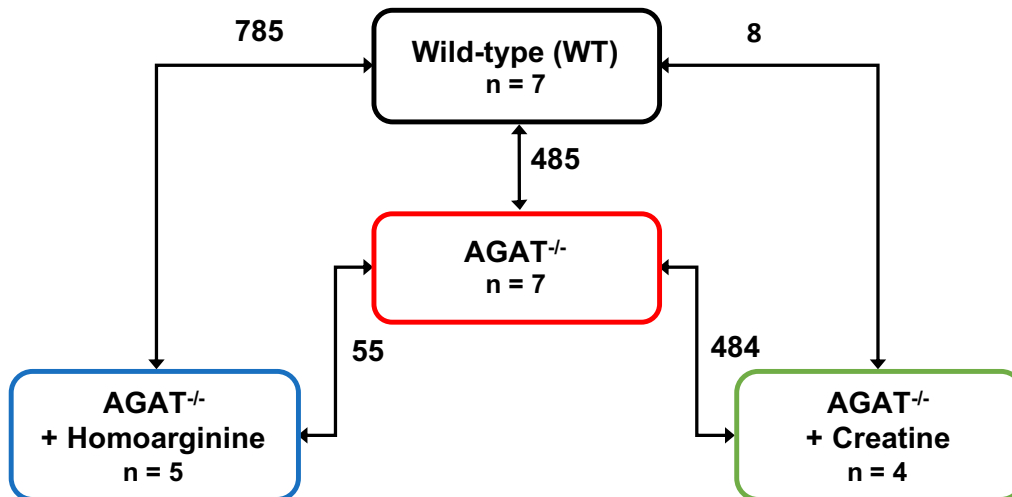


**Figure 8: Number of differentially expressed genes between the groups in murine heart tissue**
Expression profiling was performed using the Affymetrix Mouse GeneChip 1.0 ST Array. Each line indicates the comparison of two groups and the number of significantly regulated genes. Significance level: False discovery rate (FDR) ≤ 0.05. WT: wild-type; AGAT$^{-/-}$: AGAT knockout; n: number of animals.

**Wild-type versus AGAT knockout mice**

Of the 19,954 probes on the array that were included in the gene expression analysis, 485 were significantly regulated (FDR ≤ 0.05) in left ventricular heart tissue of AGAT$^{-/-}$ mice. Table 12 shows the top 20 genes that are differentially expressed between WT and AGAT$^{-/-}$ littermates. The fold change (FC) describes the change in gene expression in AGAT$^{-/-}$ compared to WT mice. Expectably, a significant down-regulation of the *Agat* gene was observed in AGAT$^{-/-}$ mice ($P$ = 1.18×10$^{-10}$, FC = -2.19). As already described, the knockout leads to a shortened instable mRNA and accordingly, the expression was significantly lower but not completely absent in AGAT$^{-/-}$ mice. The first two genes within the analysis, sodium voltage-gated channel alpha subunit 4 (*Scn4a*) and sodium voltage-gated channel beta subunit 4 (*Scn4b*) were down-regulated more than 3-fold respectively (*Scn4a* $P$ = 3.02×10$^{-13}$, FC = -3.22; *Scn4b* $P$ = 1.47×10$^{-12}$,

FC = -3.74). Both are described to be involved in cardiac rhythmicity (Lau et al., 2009, Li et al., 2013).

**Table 12: Top 20 differentially expressed genes between wild-type and AGAT knockout mice in heart tissue**
Significance level: False discovery rate (FDR) ≤ 0.05. FC: fold change.

| Gene | Gene name | P-value | FC |
|------|-----------|---------|-----|
| *Scn4a* | sodium channel, voltage-gated, type IV, alpha | $3.02×10^{-13}$ | -3.22 |
| *Scn4b* | sodium channel, type IV, beta | $1.47×10^{-12}$ | -3.74 |
| *Tmod4* | tropomodulin 4 | $8.93×10^{-11}$ | -1.76 |
| *Tmem150c* | transmembrane protein 150C | $9.97×10^{-11}$ | -2.96 |
| *Fah* | fumarylacetoacetate hydrolase | $1.08×10^{-10}$ | -2.36 |
| *Agat* | L-arginine:glycine amidinotransferase | $1.18×10^{-10}$ | -2.19 |
| *Lgi1* | leucine-rich repeat LGI family, member 1 | $2.07×10^{-10}$ | -3.1 |
| *Lad1* | ladinin | $2.63×10^{-10}$ | 2.17 |
| *Stom* | stomatin | $1.12×10^{-9}$ | -1.41 |
| *Zfp106* | zinc finger protein 106 | $1.31×10^{-9}$ | 1.49 |
| *Egf* | epidermal growth factor | $6.62×10^{-9}$ | -1.55 |
| *Ndrg4* | N-myc downstream regulated gene 4 | $9.12×10^{-9}$ | 1.44 |
| *Vwa8* | von Willebrand factor A domain containing 8 | $1.2×10^{-8}$ | -1.35 |
| *Ano5* | anoctamin 5 | $1.78×10^{-8}$ | -2.27 |
| *Slc16a7* | solute carrier family 16 member 7 | $1.97×10^{-8}$ | 1.7 |
| *Ivd* | isovaleryl coenzyme A dehydrogenase | $2.54×10^{-8}$ | -1.41 |
| *Hn1* | hematological and neurological expressed sequence 1 | $2.6×10^{-8}$ | 1.41 |
| *Nr0b2* | nuclear receptor subfamily 0, group B, member 2 | $3.93×10^{-8}$ | 1.47 |
| *Slc22a3* | solute carrier family 22 (organic cation transporter), member 3 | $3.99×10^{-8}$ | -1.66 |
| *Acsm5* | acyl-CoA synthetase medium-chain family member 5 | $4.32×10^{-8}$ | -1.88 |

Subsequently performed pathway analyses (Wikipathways, WebGestalt) within that cluster of 485 genes revealed that regulated genes were especially enriched in pathways involved in energy metabolism such as fatty acid biosynthesis (adjusted $P$ (adj. $P$) = $4.07×10^{-9}$), mitochondrial LC-fatty acid beta-oxidation (adj. $P$ = $6.78×10^{-8}$), fatty acid beta-oxidation (adj. $P$ = $1.06×10^{-7}$) and glycogen metabolism (adj. $P$ = $8.83×10^{-5}$). In particular, these energy-related genes revealed a down-regulation in AGAT$^{-/-}$ mice. More detailed, at the level of individual genes, important genes of the fatty acid oxidation such as acetyl-CoA C-acyltransferase 2 (*Acaa2*), long chain fatty acid CoA ligase 1 (*Acsl1*) or acyl-CoA dehydrogenase short chain (*Acads*) were down-regulated in response to the AGAT knockout. In addition, a relation to the cardiovascular system was found by an enrichment of genes involved in cardiac calcium regulation (adj. $P$ = $6.51×10^{-6}$). The top ten pathways including significantly regulated genes are illustrated in Figure 9.
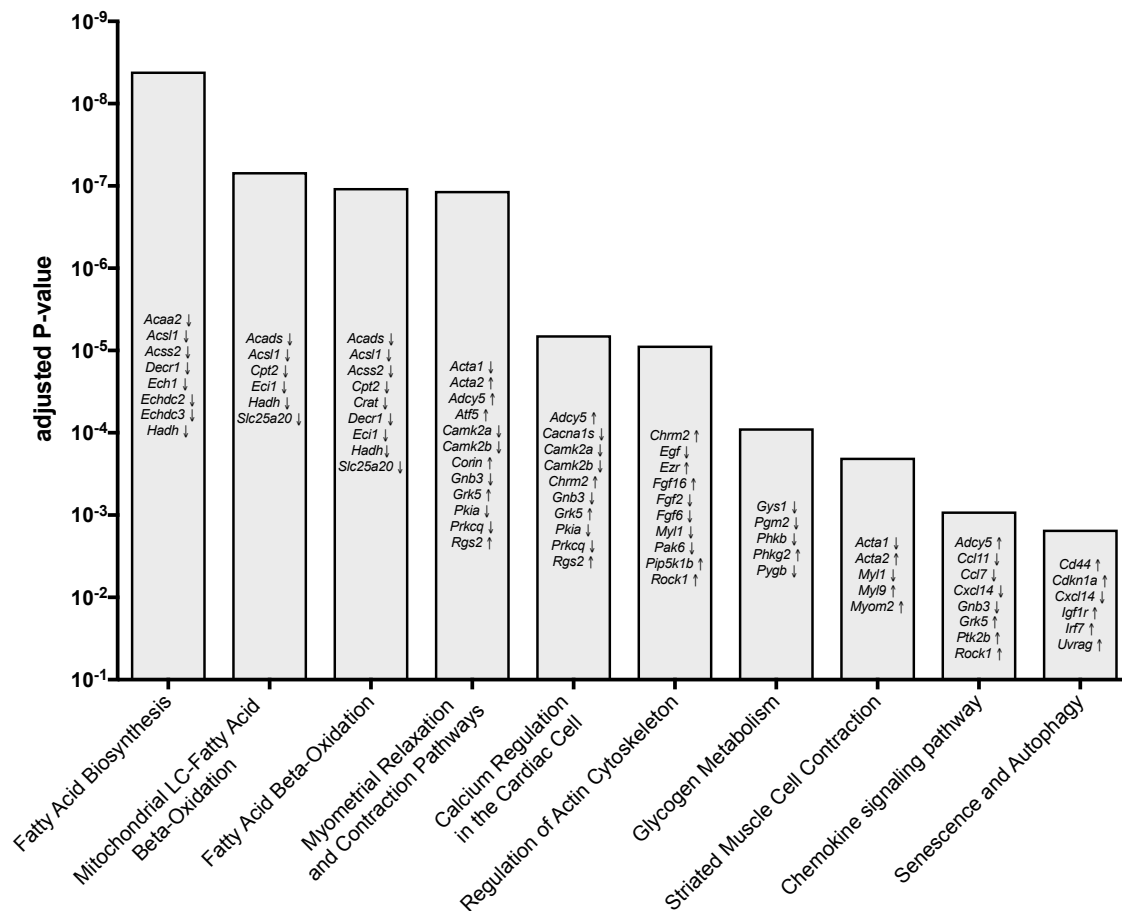
**Figure 9: Wikipathways pathway analysis within the 485 significantly regulated genes between wild-type and AGAT knockout mice in heart tissue**
The top ten pathways are shown and the involved genes are listed in the bars. The direction of regulation is indicated by up and down arrows respectively. Significance level: Adjusted P-value ≤ 0.05.

**Effects of creatine supplementation**

AGAT catalyzes the first step in creatine biosynthesis, so that AGAT$^{-/-}$ mice are deficient of creatine. In order to investigate the effects of creatine supplementation, differential gene expression analysis was performed between WT and AGAT$^{-/-}$Cr. The FC refers to the first named mouse group. Besides a 2-fold down-regulation of *Agat* only seven other genes remained significantly differentially expressed (FDR ≤ 0.05) between WT and AGAT$^{-/-}$Cr (Table 13). This indicates that only 2% of AGAT-dependent deregulated genes remained differentially expressed after creatine supplementation and gave first evidence that gene expression in AGAT$^{-/-}$ mice can be rescued by creatine supplementation. In order to further investigate this assumption, the comparison of AGAT$^{-/-}$ and AGAT$^{-/-}$Cr mice was conducted. The analysis revealed 484 significantly regulated genes between the groups. Crucially, most of the genes

also occur in the comparison of WT versus AGAT$^{-/-}$ mice but are regulated in the other direction respectively.

**Table 13: Differentially expressed genes between wild-type and creatine-supplemented AGAT knockout mice in heart tissue**
Significance level: False discovery rate (FDR) ≤ 0.05. FC: fold change.

| Gene | Gene name | P-value | FC |
|------|-----------|---------|-----|
| *Agat* | L-arginine:glycine amidinotransferase | $2.39×10^{-8}$ | -1.99 |
| *Mcm8* | minichromosome maintenance deficient 8 (S. cerevisiae) | $4.13×10^{-7}$ | -1.52 |
| *Pde1c* | phosphodiesterase 1C | $7.98×10^{-7}$ | -1.38 |
| *Mertk* | c-mer proto-oncogene tyrosine kinase | $9.01×10^{-7}$ | -1.43 |
| *Hmcn1* | hemicentin 1 | $8.26×10^{-6}$ | -1.46 |
| *Cds2* | CDP-diacylglycerol synthase 2 | $9.07×10^{-6}$ | -1.3 |
| *Rasgef1b* | RasGEF domain family, member 1B | $1.25×10^{-5}$ | -1.56 |
| *Gm14085* | predicted gene 14085 | $1.37×10^{-5}$ | 1.37 |

**Effects of homoarginine supplementation**

Additional to creatine deficiency, AGAT$^{-/-}$ mice are unable to produce homoarginine, which itself is a biomarker for poor prognosis in CVD (Atzler et al., 2015). AGAT$^{-/-}$ mice exhibit chronotropic, inotropic and lusitropic deficits *in vivo* that are completely rescued by homoarginine supplementation (Faller et al., 2017). Therefore, it was of interest to find out whether transcriptomic signatures might explain these observations. The analysis of WT and AGAT$^{-/-}$HA mice showed 785 (FDR ≤ 0.05) significantly regulated genes. Table 14 represents the selection of the 20 most significant genes. The comparison of these genes with the 485 differentially expressed genes between WT and AGAT$^{-/-}$ mice revealed that only 204 genes (i.e. 42%) could be restored by homoarginine supplementation, whereas a large proportion remained regulated or demonstrated regulation by homoarginine supplementation only.

**Table 14: Top 20 differentially expressed genes between wild-type and homoarginine-supplemented knockout mice in heart tissue**

Significance level: False discovery rate (FDR) ≤ 0.05. FC: fold change.

| Gene | Gene name | P-value | FC |
|---|---|---|---|
| *Mthfd2* | methylenetetrahydrofolate dehydrogenase (NAD+ dependent), methenyltetrahydrofolate cyclohydrolase | $4.37 \times 10^{-13}$ | 4.59 |
| *Scn4a* | sodium channel, voltage-gated, type IV, alpha | $6.63 \times 10^{-11}$ | -2.81 |
| *Agat* | L-arginine:glycine amidinotransferase | $4.92 \times 10^{-10}$ | -2.32 |
| *Wfdc1* | WAP four-disulfide core domain 1 | $6.87 \times 10^{-10}$ | -1.75 |
| *Myot* | myotilin | $7.11 \times 10^{-10}$ | -2.88 |
| *Tmem150c* | transmembrane protein 150C | $8.76 \times 10^{-10}$ | -2.94 |
| *Lgi1* | leucine-rich repeat LGI family, member 1 | $9.99 \times 10^{-10}$ | -4.27 |
| *Lad1* | ladinin | $2.23 \times 10^{-9}$ | 2.42 |
| *Fah* | fumarylacetoacetate hydrolase | $3.36 \times 10^{-9}$ | -2.33 |
| *Slc16a7* | solute carrier family 16 (monocarboxylic acid transporters), member 7 | $4.54 \times 10^{-9}$ | 1.75 |
| *Stom* | stomatin | $7.04 \times 10^{-9}$ | -1.46 |
| *Asns* | asparagine synthetase | $7.21 \times 10^{-9}$ | 2.97 |
| *Atf5* | activating transcription factor 5 | $7.45 \times 10^{-9}$ | 2.02 |
| *Slc7a5* | solute carrier family 7 (cationic amino acid transporter, y+ system), member 5 | $3.38 \times 10^{-8}$ | 1.75 |
| *Amot* | angiomotin | $5.25 \times 10^{-8}$ | -1.52 |
| *Scn4b* | sodium channel, type IV, beta | $6.13 \times 10^{-8}$ | -3.34 |
| *Tmod4* | tropomodulin 4 | $6.27 \times 10^{-8}$ | -1.74 |
| *Aldh1l2* | aldehyde dehydrogenase 1 family, member L2 | $6.98 \times 10^{-8}$ | 1.98 |
| *Ttc12* | tetratricopeptide repeat domain 12 | $7.23 \times 10^{-8}$ | 1.38 |
| *Ivd* | isovaleryl coenzyme A dehydrogenase | $1.11 \times 10^{-7}$ | -1.53 |

### 5.1.4 Selection of candidate genes for subsequent analyses

**Network analysis and known association to cardiovascular disease**

In order to further investigate AGAT-related molecular mechanisms that might cause the cardiovascular phenotype in AGAT$^{-/-}$ mice, candidate genes were selected within the significantly regulated genes between WT and AGAT$^{-/-}$ littermates. To that end, a two-step approach was carried out: To find clusters of highly co-expressed genes, network analyses within the 485 significantly regulated genes were performed. Subsequently, the two networks with the strongest associations ($P = 1.07 \times 10^{-8}$ and $P = 4.39 \times 10^{-8}$) were used to identify candidate genes based on known association to the cardiovascular system and a strong connectivity to other genes (Figure 10). Within the most significant networks, *Scn4a* and *Scn4b* seem to play a pivotal role, moreover, the appearance of connective tissue growth factor (*Ctgf*), hyperpolarization-activated cyclic nucleotide-gated ion channel 2 and 4 (*Hcn2* and *Hcn4*), natriuretic peptide type A (*Nppa*) and uncoupling protein 2 (*Ucp2*) was remarkable since they were

already linked to the cardiovascular system. Therefore, these genes were selected for further characterization. Table 15 gives an overview of literature-based research on these cardiovascular candidate genes.
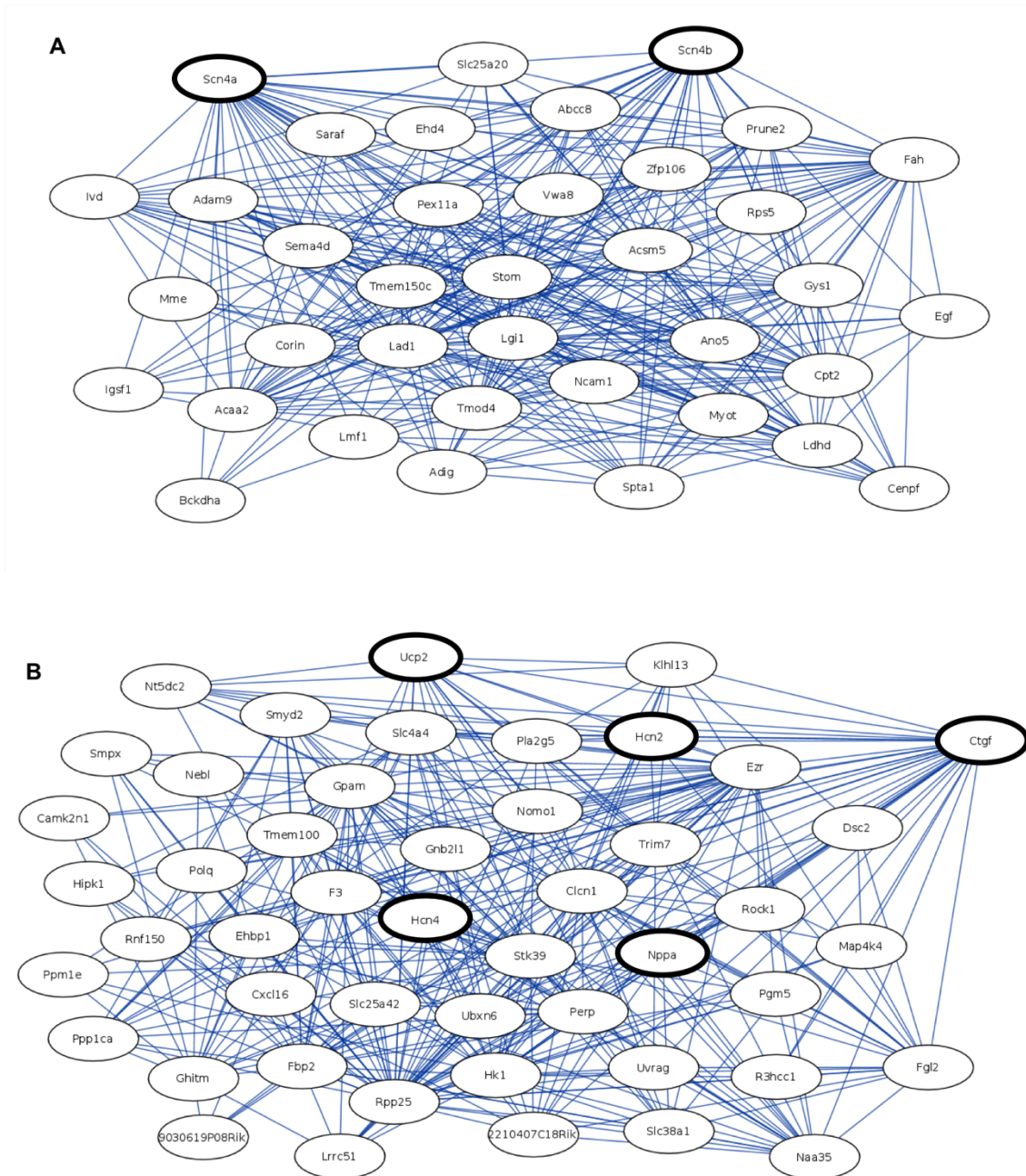


**Figure 10: Network analysis between wild-type and AGAT knockout mice in heart tissue**
Genes were clustered into modules of highly co-expressed genes. The networks with the strongest associations are shown (**A**, *P* = 1.07×10⁻⁸; **B**, *P* = 4.39×10⁻⁸). Candidate genes (black circles) were selected based on known association to the cardiovascular system and strong connectivity to other genes.

**Table 15: Differentially expressed cardiovascular candidate genes between wild-type and AGAT knockout mice in heart tissue**
Candidate genes were identified by network analysis and known association to the cardiovascular system.

| Gene | Gene name | Association to the cardiovascular system |
| --- | --- | --- |
| *Scn4a* | sodium channel, voltage-gated, type IV, alpha | Antiarrhythmic properties (Lau et al., 2009), preserved normal conduction in murine hearts after MI (Coronel et al., 2010) |
| *Scn4b* | sodium channel, type IV, beta | Associated to atrial fibrillation (Li et al., 2013) and Long QT syndrome (Medeiros-Domingo et al., 2007) |
| *Ucp2* | uncoupling protein 2 | Regulator of lipid metabolism, control of mitochondria-derived reactive oxygen species (Saleh et al., 2002) |
| *Ctgf* | connective tissue growth factor | Up-regulated in cardiac myocytes and fibroblasts after MI (Ohnishi et al., 1998), in heart failure (Ahmed et al., 2004) and atherosclerosis (Oemar et al., 1997) |
| *Nppa* | natriuretic peptide type A | Biomarker for heart failure and atrial fibrillation (Wang et al., 2004) |
| *Hcn2* | hyperpolarization-activated cyclic nucleotide-gated ion channel 2 | Spontaneous rhythmic activity in heart and brain (Vaccari et al., 1999) |
| *Hcn4* | hyperpolarization-activated cyclic nucleotide-gated ion channel 4 | Control of rhythmic activity of the heart (DiFrancesco, 2010), associated to atrial fibrillation and sudden cardiac death (Baruscotti et al., 2010), bradycardia in mice (Baruscotti et al., 2011) |

Furthermore, it was of interest whether creatine and homoarginine supplementation showed a regulatory effect on the expression of *Scn4a*, *Scn4b*, *Ucp2*, *Ctgf*, *Nppa*, *Hcn2* and *Hcn4*. The analysis revealed that the expression of these genes is regulated by creatine supplementation (Table 16). The FC for the comparison of AGAT$^{-/-}$ and AGAT$^{-/-}$Cr littermates indicates a regulation to the opposite direction when comparing with the corresponding FC for WT and AGAT$^{-/-}$ mice. In contrast, the analysis of AGAT$^{-/-}$ and AGAT$^{-/-}$HA mice showed no significant differential expression of these genes suggesting that homoarginine supplementation has no regulatory effects.

**Table 16: Gene expression in the heart restored by creatine supplementation**
Differential gene expression of cardiovascular candidate genes between wild-type (WT) and AGAT knockout mice (AGAT$^{-/-}$) was compared with the differential expression of these genes between AGAT$^{-/-}$ and creatine-supplemented AGAT$^{-/-}$ (AGAT$^{-/-}$Cr) or homoarginine-supplemented AGAT$^{-/-}$ (AGAT$^{-/-}$HA) mice. Significance level: False discovery rate (FDR) ≤ 0.05. FC: fold change.

| Gene | Gene name | WT vs. AGAT$^{-/-}$ | | AGAT$^{-/-}$ vs. AGAT$^{-/-}$Cr | | AGAT$^{-/-}$ vs. AGAT$^{-/-}$HA | |
|------|-----------|---------|-----|---------|-----|---------|-----|
| | | P-value | FC | P-value | FC | P-value | FC |
| *Scn4a* | sodium channel, type IV, alpha | $3.02×10^{-13}$ | -3.22 | $6.24×10^{-10}$ | 2.85 | ns | 1.15 |
| *Scn4b* | sodium channel, type IV, beta | $1.47×10^{-12}$ | -3.74 | $5.81×10^{-12}$ | 4.21 | ns | 1.12 |
| *Ucp2* | uncoupling protein 2 | $3.49×10^{-7}$ | 1.85 | $2.55×10^{-6}$ | -2.09 | ns | -1.2 |
| *Ctgf* | connective tissue growth factor | $5.21×10^{-7}$ | 1.78 | $1.94×10^{-6}$ | -2.36 | ns | 1.03 |
| *Nppa* | natriuretic peptide type A | $1.17×10^{-5}$ | 1.93 | $3.92×10^{-4}$ | -1.89 | ns | -1.24 |
| *Hcn2* | hyperpolarization-activated cyclic nucleotide-gated ion channel 2 | $1.48×10^{-5}$ | 1.33 | $9.56×10^{-7}$ | -1.55 | ns | -1.11 |
| *Hcn4* | hyperpolarization-activated cyclic nucleotide-gated ion channel 4 | $2.93×10^{-4}$ | -1.42 | $1.7×10^{-3}$ | 1.32 | ns | 1.1 |

**Gene expression restored by homoarginine supplementation**

AGAT$^{-/-}$ mice exhibit cardiac dysfunction, which was corrected completely by supplementation of homoarginine. As described above, the expression of CVD-related candidate genes was restored by creatine supplementation. Therefore, the goal was to identify other genes whose expression was dependent on homoarginine.

When comparing WT versus AGAT$^{-/-}$ and AGAT$^{-/-}$ versus AGAT$^{-/-}$HA and taking an opposite regulation as selection criterion, the expression of only five genes, beta-1,4-galactosyltransferase 6 (*B4galt6*), collagen and calcium binding EGF domains 1 (*Ccbe1*), chemokine (C-C motif) ligand 11 (*Ccl11*), cyclin-dependent kinase inhibitor 1A (*Cdkn1a*), phosphatidylinositol-4-phosphate 5-kinase type 1 beta (*Pip5k1b*), was identified to be restored by homoarginine supplementation (Table 17). For this reason, these genes were selected as candidates for further analysis. With the exception of *Ccl11,* which might be implicated in atherosclerosis (Haley et al., 2000, Wang et al., 2013), an association of the other four genes to the cardiovascular system has not been described so far.

**Table 17: Gene expression in the heart restored by homoarginine supplementation**
Differentially expressed genes between wild-type (WT) versus AGAT knockout (AGAT$^{-/-}$) and AGAT$^{-/-}$ versus homoarginine-supplemented AGAT$^{-/-}$ (AGAT$^{-/-}$HA) mice but regulated in the other direction were evaluated. The third column of the table shows the according data for the comparison of AGAT$^{-/-}$ versus creatine-supplemented AGAT$^{-/-}$ (AGAT$^{-/-}$Cr) littermates. Significance level: False discovery rate (FDR) ≤ 0.05. FC: fold change.

| Gene | Gene name | WT vs. AGAT$^{-/-}$ | | AGAT$^{-/-}$ vs. AGAT$^{-/-}$HA | | AGAT$^{-/-}$ vs. AGAT$^{-/-}$Cr | |
|------|-----------|---------|-----|---------|-----|---------|-----|
| | | P-value | FC | P-value | FC | P-value | FC |
| *Ccl11* | chemokine (C-C motif) ligand 11 | $1.32 \times 10^{-6}$ | -1.68 | $1.37 \times 10^{-5}$ | 1.57 | ns | 1.15 |
| *Ccbe1* | collagen and calcium binding EGF domains 1 | $3.60 \times 10^{-5}$ | -1.68 | $7.29 \times 10^{-5}$ | 1.51 | $1.32 \times 10^{-4}$ | 1.59 |
| *Cdkn1a* | cyclin-dependent kinase inhibitor 1A (P21) | $6.67 \times 10^{-5}$ | 2.32 | $6.13 \times 10^{-6}$ | -2 | $4.63 \times 10^{-6}$ | -2.65 |
| *Pip5k1b* | phosphatidylinositol -4-phosphate 5-kinase, type 1 beta | $6.87 \times 10^{-5}$ | 1.41 | $2.19 \times 10^{-6}$ | -1.35 | $2.45 \times 10^{-7}$ | -1.5 |
| *B4galt6* | beta-1,4-galactosyltransfera se 6 | $6.43 \times 10^{-4}$ | 1.23 | $9.78 \times 10^{-5}$ | -1.32 | $4.09 \times 10^{-6}$ | -1.42 |

## 5.1.5 Validation of candidate genes

**Validation on mRNA level by qPCR**

To validate the candidate genes identified by microarray analysis, total RNA was reverse transcribed into cDNA and used as a template for qPCR. Each sample was analyzed in duplicates and normalized to an endogenous control (18S rRNA). Figure 11 shows the mRNA expression of the seven cardiovascular candidate genes. According to the microarray results, the mRNA level of *Scn4a*, *Scn4b* and *Hcn4* was lower in the AGAT$^{-/-}$ and AGAT$^{-/-}$HA group compared to WT, whereas no major difference was observed for the comparison of AGAT$^{-/-}$Cr and WT littermates. *Ucp2*, *Ctgf*, *Nppa* and *Hcn2* revealed an up-regulation in the AGAT$^{-/-}$ and AGAT$^{-/-}$HA group compared to WT. Remarkably, again no significant difference in mRNA expression was seen between WT and AGAT$^{-/-}$Cr mice.

The validation of candidate genes identified based on restored gene expression by homoarginine supplementation showed significant up-regulation of *B4galt6*, *Pip5k1b* and *Cdkn1a* and a down-regulation of *Ccbe1* and *Ccl11* in AGAT$^{-/-}$ compared to WT mice on mRNA level. As expected, homoarginine supplementation adapted the mRNA levels of AGAT$^{-/-}$ to the WT group. No difference was also observed between WT and AGAT$^{-/-}$Cr mice (Figure 12).
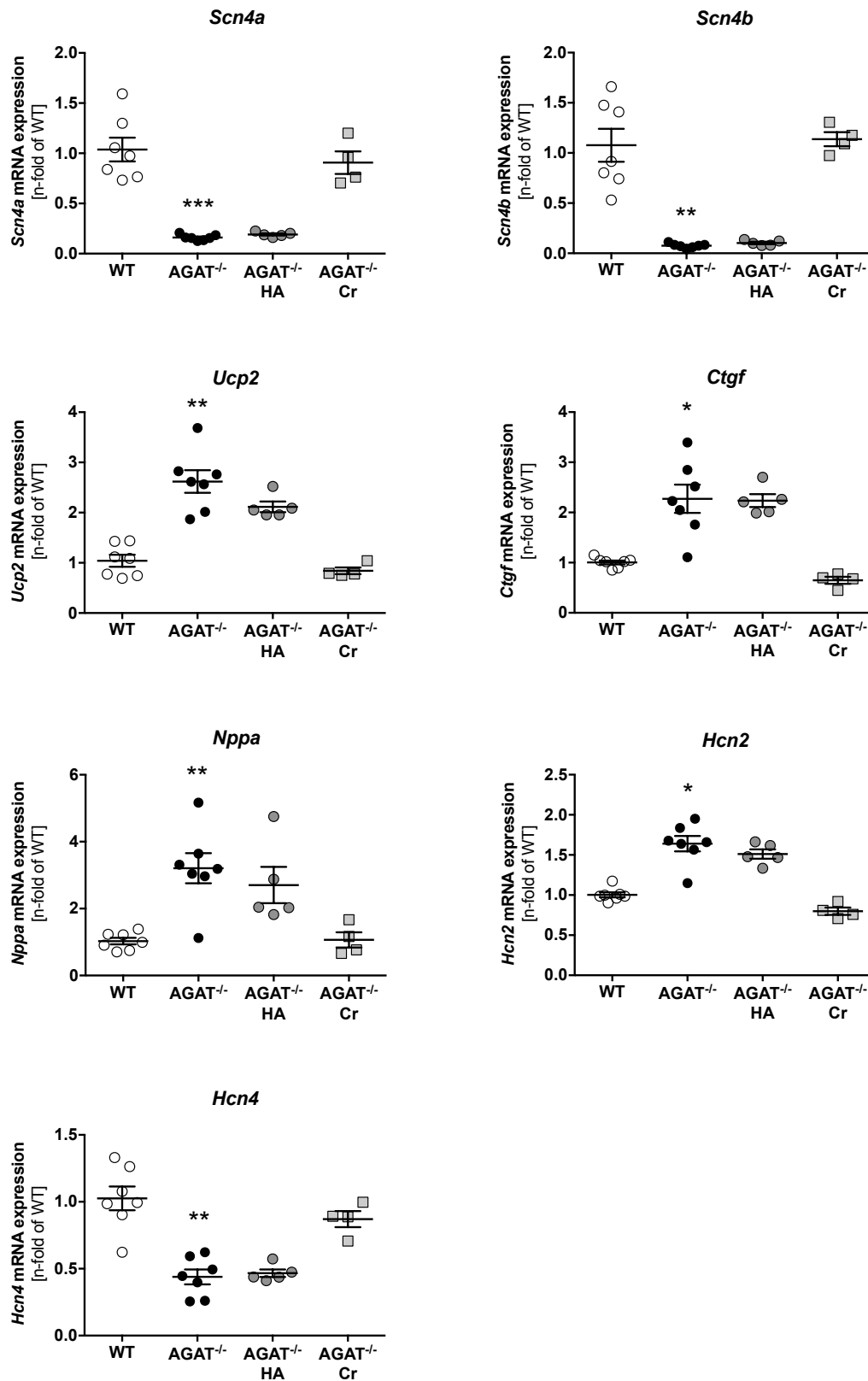
**Figure 11: Validation of cardiovascular candidate genes by qPCR**
Relative mRNA expression of candidate genes in the heart identified based on network analysis and known association to the cardiovascular system. Values are expressed as mean ± SEM. * $P < 0.05$; ** $P < 0.01$ and *** $P < 0.001$ versus wild-type (WT), Kruskal-Wallis-Test. WT (n = 7), AGAT knockout (AGAT$^{-/-}$; n = 7), homoarginine-supplemented AGAT$^{-/-}$ (AGAT$^{-/-}$HA; n = 5), creatine-supplemented AGAT$^{-/-}$ (AGAT$^{-/-}$Cr; n = 4).
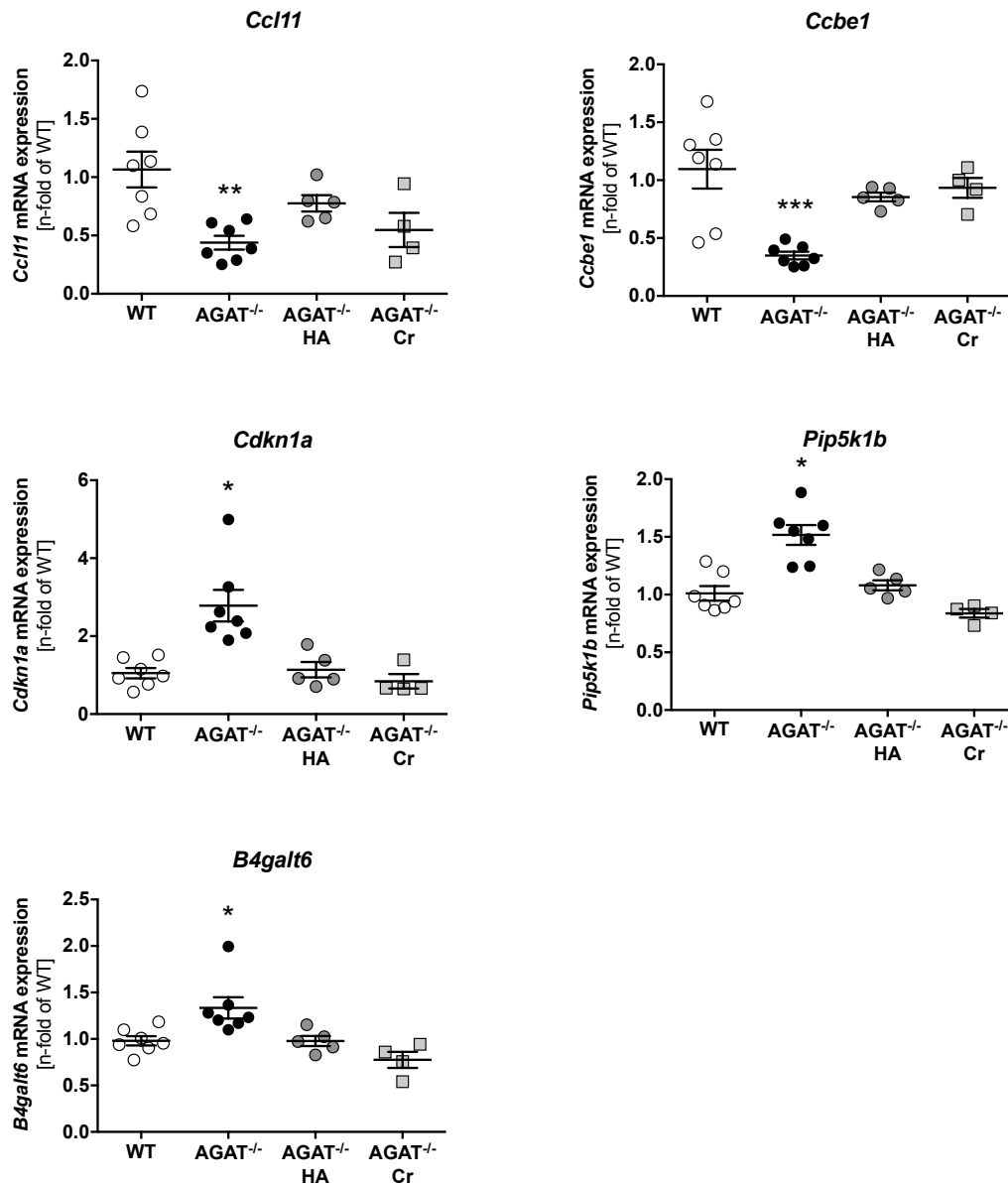
**Figure 12: Validation of homoarginine-dependent candidate genes by qPCR**
Relative mRNA expression of candidate genes in the heart identified based on restored expression by homoarginine supplementation. Values are expressed as mean ± SEM. * $P < 0.05$; ** $P < 0.01$ and *** $P < 0.001$ versus wild-type (WT), Kruskal-Wallis-Test. WT (n = 7), AGAT knockout (AGAT$^{-/-}$; n = 7), homoarginine-supplemented AGAT$^{-/-}$ (AGAT$^{-/-}$HA; n = 5), creatine-supplemented AGAT$^{-/-}$ (AGAT$^{-/-}$Cr; n = 4).

**Validation on protein level by western blot**

Left ventricular heart tissue of AGAT mice was used for western blot analysis in order to investigate the expression of the candidate genes on protein level. No results were achieved for ANP, B4GALT6, CCBE1, CCL11, HCN2, HCN4, PIP5K1B, SCN4A and SCN4B expression due to low expression or because antibody-based detection failed. Results are shown for CTGF, CDKN1A and UCP2 (Figure 13). Whereas transcriptomic analysis showed an up-regulation of *Ctgf* on mRNA level, this finding could not be validated on protein expression level. There were no differences between the four groups of mice. Overall, CDKN1A protein expression within the groups was very low. A higher expression was detected in AGAT$^{-/-}$ mice, but the quantification indicated no difference between the groups. The analysis of cardiac UCP2 protein expression revealed a trend towards a higher level of expression in AGAT$^{-/-}$ compared to WT mice, which was consistent with the mRNA expression profile. Nevertheless, the described finding was not statistically significant.
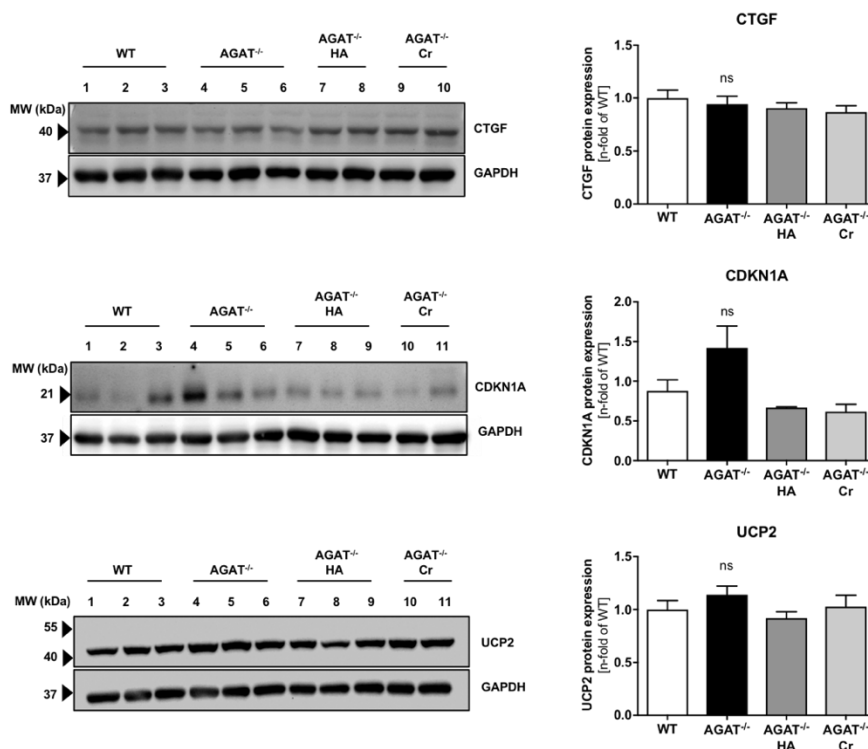


**Figure 13: Protein expression of CDKN1A, CTGF and UCP2 in murine heart tissue**
Representative western blots of protein expression in wild-type (WT), AGAT knockout (AGAT$^{-/-}$), homoarginine-supplemented AGAT$^{-/-}$ (AGAT$^{-/-}$HA) and creatine-supplemented AGAT$^{-/-}$ (AGAT$^{-/-}$Cr) mice. Arrowheads indicate the molecular weights. GAPDH was used as a loading control. On the right side quantitative analysis of protein expression respectively. Values are normalized to GAPDH and expressed as mean ± SEM related to WT, Kruskal-Wallis-Test. MV: molecular weight; ns: not significant.

## 5.2 Analysis of AGAT-related miRNA expression in the heart

Latest research increasingly focuses on miRNAs as regulator and biomarker in CVD (Romaine et al., 2015, Schulte and Zeller, 2015). Therefore, another aim of this study was to characterize the miRNA expression profile within the different mouse groups (WT, AGAT$^{-/-}$ and AGAT$^{-/-}$HA; 5 mice per group). RNA of left ventricular heart tissue was isolated using the QIAzol/chloroform extraction method, which ensures the preservation of the miRNA fraction. After preparation of the miRNA library, next-generation sequencing was carried out using the Illumina sequencing system. The following part shows the differentially expressed mature miRNAs whereby the suffix 3p and 5p indicates the origin of the miRNA from the 3' arm or 5' arm respectively.

### 5.2.1 Differential miRNA expression in AGAT knockout mice

The number of differentially expressed miRNAs between WT, AGAT$^{-/-}$ and AGAT$^{-/-}$HA was evaluated for each comparison as shown in Figure 14. After correction for multiple testing, the FDR was set to ≤ 0.05.
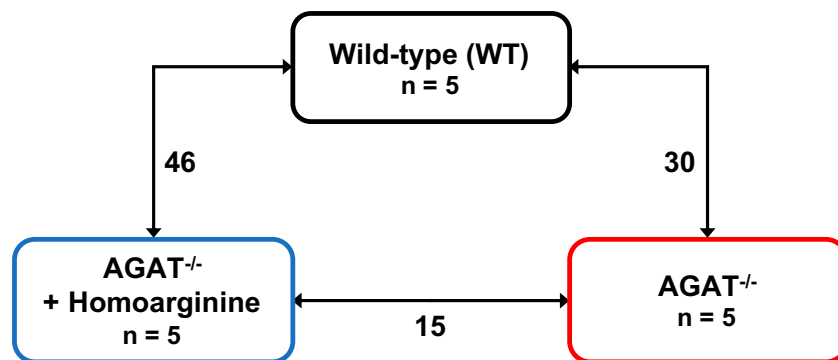


**Figure 14: Number of differentially expressed miRNAs between the groups in murine heart tissue**
Expression profiling was carried out using the Illumina sequencing system. Each line indicates the comparison of two groups with the associated number of differentially expressed miRNAs. Significance level: False discovery rate (FDR) ≤ 0.05. WT: wild-type; AGAT$^{-/-}$: AGAT knockout; n: number of animals.

**Wild-type versus AGAT knockout mice**

Out of 953 detected miRNAs, 30 were significantly differentially expressed between WT and AGAT$^{-/-}$ mice (FDR ≤ 0.05). Among the 30 miRNAs, 19 were up-regulated and eleven miRNAs revealed a down-regulation in AGAT$^{-/-}$ compared to WT littermates. Figure 15 illustrates the relative miRNA expression

difference between the groups. Interestingly, more than half of the miRNAs showed a regulation less than 50%.
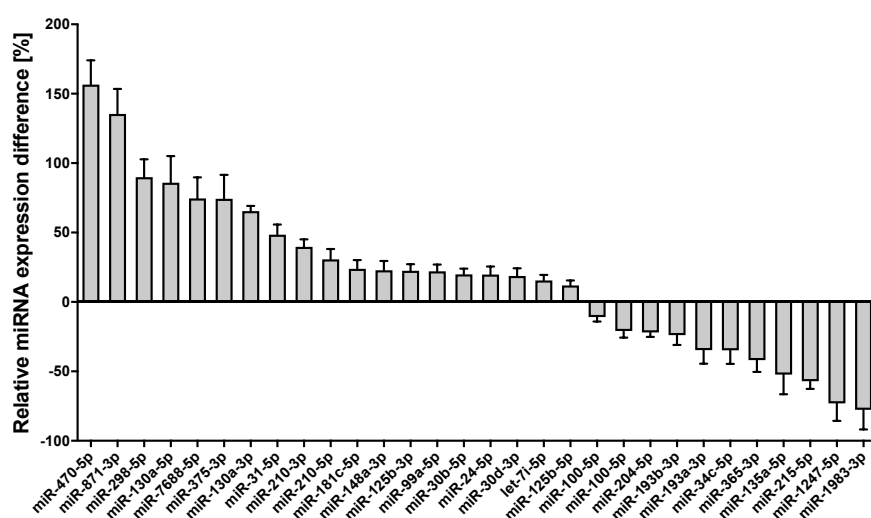


**Figure 15: Differentially expressed miRNAs between wild-type and AGAT knockout mice in heart tissue**
Mature miRNAs are shown. 3p and 5p indicates the origin of the miRNA from the 3' arm or 5' arm respectively. Values are expressed as mean ± SEM and regulation is shown in percentage compared to wild-type. Significance level: False discovery rate (FDR) ≤ 0.05.

**Effects of homoarginine supplementation**

In order to investigate homoarginine-dependent effects on the miRNA expression, two comparisons as shown in Figure 14 were carried out. Of the 953 detected miRNAs, 46 were significantly regulated between WT and AGAT$^{-/-}$HA mice (Figure 16 A). 26 miRNAs were up-regulated whereas the remaining 20 revealed a down-regulation compared to WT. Eight significantly regulated miRNAs in the comparison of WT and AGAT$^{-/-}$ did not remain differentially expressed between WT and AGAT$^{-/-}$HA mice (miR-34c, miR-135a, miR-148a, miR-181c, miR-193b, miR-871, miR-7688, let-7i).

Figure 16 B shows the 15 differentially expressed miRNAs between AGAT$^{-/-}$ and AGAT$^{-/-}$HA. It was of interest that in both analyses (WT versus AGAT$^{-/-}$HA and AGAT$^{-/-}$ versus AGAT$^{-/-}$HA) miR-301b, miR-378b and miR-3969 seem to play an important role. These miRNAs demonstrated the smallest P-value and strongest miRNA expression difference. A regulation has not been observed in association with the AGAT knockout since no significant difference occurred between WT and AGAT$^{-/-}$ littermates. Thus, the regulation is exclusively attributable to homoarginine supplementation.

**A**



**B**



**Figure 16: Differentially expressed miRNAs between the groups of mice in heart tissue A,** Between wild-type (WT) and homoarginine-supplemented AGAT knockout mice (AGAT$^{-/-}$HA) and **B**, between AGAT knockout (AGAT$^{-/-}$) and AGAT$^{-/-}$HA in heart tissue. Mature miRNAs are shown. 3p and 5p indicates the origin of the miRNA from the 3' arm or 5' arm respectively. Values are expressed as mean ± SEM and regulation is shown in percentage compared to WT (WT versus AGAT$^{-/-}$HA) or AGAT$^{-/-}$ (AGAT$^{-/-}$ versus AGAT$^{-/-}$HA). Significance level: False discovery rate (FDR) ≤ 0.05.

## 5.2.2  Selection of candidate miRNAs

To identify candidate miRNAs that might influence the cardiovascular system, literature-based research within the 30 differentially expressed miRNAs between WT and AGAT$^{-/-}$ mice was carried out. Out of the 30 miRNAs, miR-130a, miR-210, miR-204, miR-30b, miR-125b, miR-100, let-7i, miR-181c and miR-30d were already linked to the cardiovascular system. Therefore, these miRNAs were selected for further analysis. Table 18 shows the nine miRNAs and their role in CVD. Of note, transcriptomic data indicate that the expression of miR-181c and let-7i might be normalized towards the WT by homoarginine supplementation

since they did not remain significantly regulated within the comparison of WT and AGAT$^{-/-}$HA.

**Table 18: Candidate miRNAs in murine heart tissue**
Differentially expressed candidate miRNAs between wild-type and AGAT knock-out mice in heart tissue were selected based on known association to the cardiovascular system. FC: fold change.

| miRNA | Association to the cardiovascular system | P-value | FC |
|---|---|---|---|
| miR-130a | Cardiac arrhythmias (Osbourne et al., 2014), proliferation of smooth muscle cells in hypertension (Wu et al., 2011) | $3.61 \times 10^{-42}$ | 1.65 |
| miR-210 | Linked to the hypoxia pathway (Han et al., 2011), overexpressed in cells affected by CVD (Mutharasan et al., 2011) | $3.67 \times 10^{-10}$ | 1.4 |
| miR-204 | Calcification of vascular smooth muscle cells (Cui et al., 2012) | $8.53 \times 10^{-10}$ | -1.22 |
| miR-30b | Cardiac hypertrophy (He et al., 2013) | $4.56 \times 10^{-6}$ | 1.2 |
| miR-125b | Calcification of vascular smooth muscle cells (Goettsch et al., 2011) | $9.26 \times 10^{-6}$ | 1.23 |
| miR-100 | Cardiovascular homeostasis by regulating natriuretic peptides (Wong et al., 2015) | $4.13 \times 10^{-5}$ | -1.21 |
| let-7i | Highly expressed in the cardiovascular system and involved in CVD such as dilated cardiomyopathy (Satoh et al., 2011, Bao et al., 2013) | $1.75 \times 10^{-4}$ | 1.16 |
| miR-181c | Role in heart failure by targeting the mitochondrial genome (Das et al., 2014) | $5.75 \times 10^{-4}$ | 1.24 |
| miR-30d | Heart failure therapy response (Melman et al., 2015) | $1.14 \times 10^{-3}$ | 1.19 |

### 5.2.3  Validation of candidate miRNAs by qPCR

A validation of the candidate miRNAs was performed by qPCR. Therefore, total RNA including the miRNA fraction from murine left ventricular heart tissue was reverse transcribed using Small RNA TaqMan® Assays. This design allows the construction of a specific cDNA for every miRNA. Each sample was analyzed in triplicates and normalized to an endogenous control. Two different small RNAs were tested in order to find a suitable control. Applied Biosystems recommended snoRNA202 for normalization of murine miRNA expression (Wong et al., 2007) and miR-192 was tested since it was not significantly regulated and highly expressed within the sequencing experiment. Preliminary tests revealed that snoRNA202 is consistently expressed among the different groups. In contrast, the qPCR showed that miR-192 was significantly down-regulated in creatine-supplemented mice and therefore cannot be used in the following validation (Figure 17).
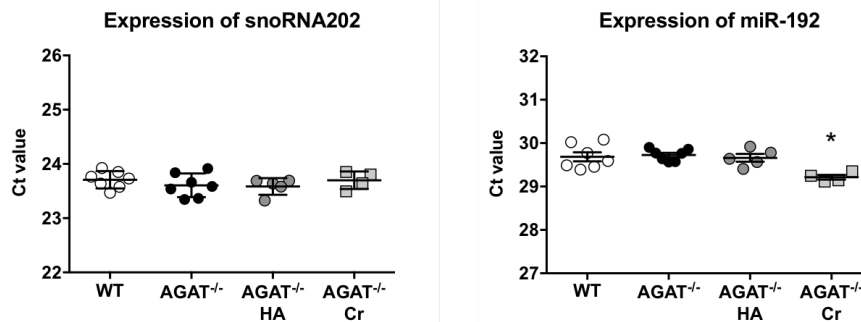
**Figure 17: Expression of snoRNA202 and miR-192 among the different mouse groups in heart tissue measured by qPCR**
Expression was measured in wild-type (WT; n = 7), AGAT knock-out (AGAT$^{-/-}$; n = 7), homoarginine-supplemented AGAT$^{-/-}$ (AGAT$^{-/-}$HA; n = 5) and creatine-supplemented AGAT$^{-/-}$ (AGAT$^{-/-}$Cr, n = 4) mice. 3p and 5p indicates the origin of the miRNA from the 3' arm or 5' arm respectively. Values are expressed as mean ± SEM. * $P < 0.05$ versus WT, Kruskal-Wallis-Test.

Additionally, this approach was used to investigate creatine-dependent effects, since this group was not included in the miRNA sequencing. Figure 18 shows the qPCR results for five of the nine candidate miRNAs. No overall expression difference between the groups was observed for miR-30b, miR-100, miR-125b and let-7i. The analysis of miR-30d, miR-130a, miR-204, miR-210 and miR-181c revealed the same expression pattern of the three groups (WT, AGAT$^{-/-}$, AGAT$^{-/-}$HA) as detected in the sequencing. Interestingly, as already expected from the sequencing results, miR-181c expression might be restored by homoarginine supplementation. However, statistical significance between WT and AGAT$^{-/-}$ was only observed for miR-204.
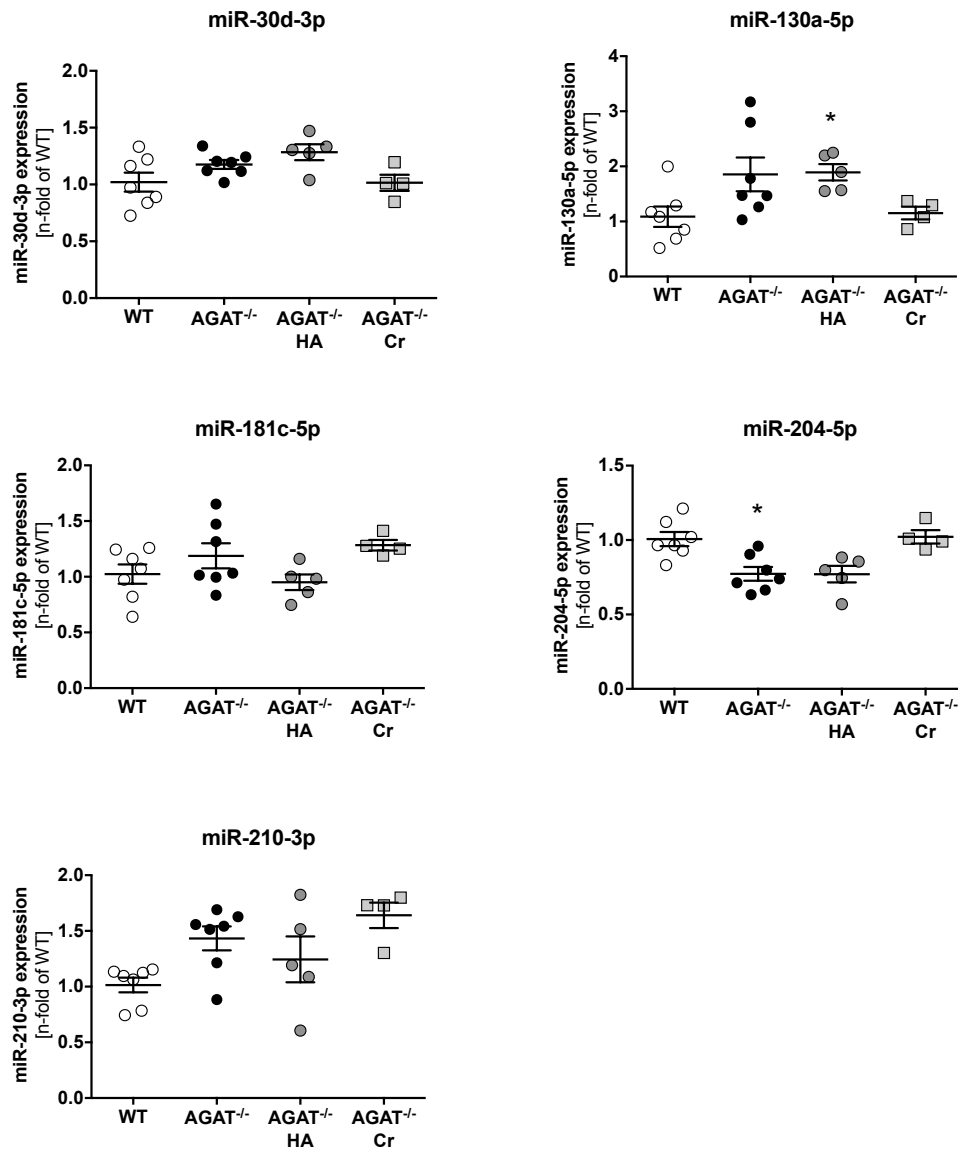
**Figure 18: Validation of selected miRNAs in the heart by qPCR**
Relative miRNA expression was measured in wild-type (WT; n = 7), AGAT knockout (AGAT$^{-/-}$; n = 7), homoarginine-supplemented AGAT$^{-/-}$ (AGAT$^{-/-}$HA; n = 5) and creatine-supplemented AGAT$^{-/-}$ (AGAT$^{-/-}$Cr; n = 4) mice. 3p and 5p indicates the origin of the miRNA from the 3' arm or 5' arm respectively. Values are expressed as mean ± SEM. * $P < 0.05$ versus WT, Kruskal-Wallis-Test.

## 5.3 mRNA-miRNA interactions

In order to combine mRNA and miRNA data, *in silico* analyses of potential miRNA binding sites were performed using the online tool miRDB (www.mirdb.org/miRDB). As a first step, all potential targets of the 30 differentially expressed miRNAs between WT and AGAT$^{-/-}$ mice were evaluated. mRNA-miRNA interactions with a target prediction score > 80 were assumed to be real and included in the analysis. Subsequently, the 485 significantly regulated genes between WT and AGAT$^{-/-}$ were aligned with the predicted targets of the miRNAs. 13 out of the 30 significantly regulated miRNAs between WT and AGAT$^{-/-}$ mice might regulate the expression of differentially expressed genes from transcriptomic analysis (Figure 19). It was of interest that miR-30b, miR-34c, miR-130a, miR-298, miR-181c, miR-204 and let-7i seem to regulate larger groups of genes. However, subsequent analysis that was performed to evaluate an enrichment of the regulated genes in molecular pathways showed no results. Notably, the candidate miRNAs associated to the cardiovascular system miR-30b, miR-30d, miR-125b, miR-130a, miR-204, miR-181c and let-7i also appeared in this context. Further analysis regarding the interaction of miRNAs and mRNAs revealed that miR-30b, miR-30d, miR-125b and let-7i might regulate the expression of previously described AGAT-related candidate genes (5.1.4). More detailed, *B4galt6* mRNA has a predicted binding site for miR-30b and miR-30d. *Scn4a* mRNA is a potential target for miR-125b and *Scn4b* mRNA might be regulated by let-7i. In addition, looking-up validated targets for miRNAs in the online database miRTarBase (http://mirtarbase.mbc.nctu.edu.tw) showed that *Ucp2* has already been identified as a target for miR-210. Of note, miR-30b, miR-181c and let-7i were also predicted to regulate the *Agat* gene.
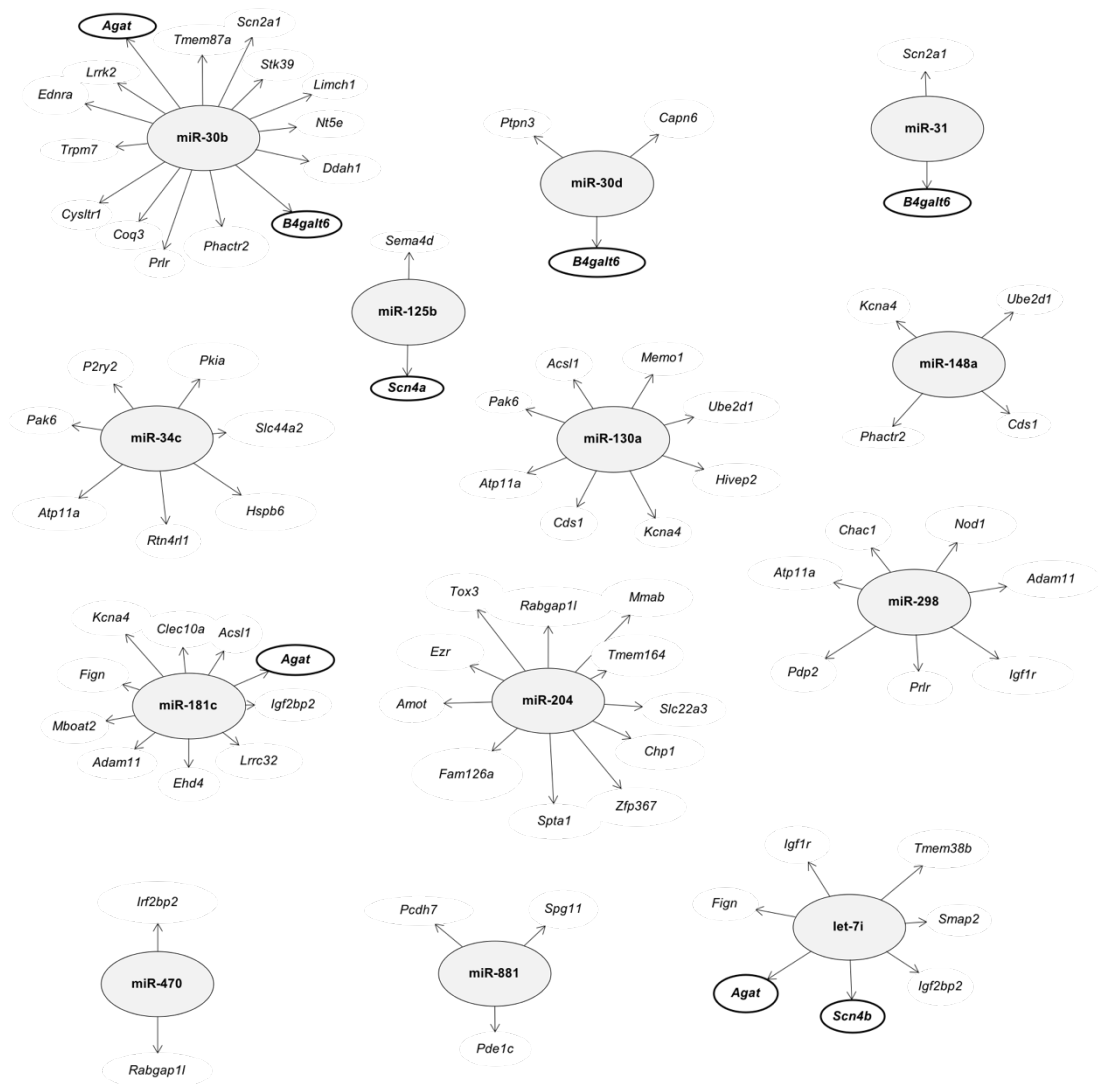
**Figure 19: miRNAs differentially expressed between wild-type and AGAT knockout mice in heart tissue and significantly regulated genes as a predicted target**
The analysis was performed using the online tool miRDB (Wong & Wang 2015). Predicted targets of the miRNAs were considered as real when a prediction score > 80 was observed. Candidate genes identified by transcriptome analysis and *Agat* are circled in black.

## 5.4 Translation into a disease model of myocardial infarction

It has been described before that low homoarginine due to an altered activity of AGAT predicts the prognosis of cardiovascular patients, amongst others, in patients with acute chest pain (Atzler et al., 2016). Since not all candidate genes have been linked to CVD, the expression of *B4galt6*, *Ccbe1*, *Ccl11*, *Cdkn1a*, *Ctgf*, *Hcn2*, *Hcn4*, *Nppa*, *Pip5k1b*, *Ucp2*, *Scn4a* and *Scn4b* was investigated in a mouse model of MI. Therefore, a two-step approach was carried out. At first, a qPCR analysis was conducted five days after MI. Subsequently*, in silico* analyses using the online database GEO were carried out to evaluate additional time points after MI and to validate the qPCR results. The aim of this analysis was to evaluate whether a regulation can be observed and this together with a regulation caused by the AGAT knockout might be a hint to decreased survival.

### 5.4.1 Analysis of candidate genes after myocardial infarction by qPCR

To investigate the role of candidate genes in CVD, the expression was measured in a mouse model of MI by qPCR. Therefore, cDNA from C57BL/6J WT mice five days after MI was kindly provided by Prof. Dr. Dirk Westermann and PD Dr. Diana Lindner (Clinic for General and Interventional Cardiology, University Heart Centre Hamburg). All samples were measured in duplicates and were normalized to an endogenous control (18S rRNA). The tissue samples of the left ventricle of sham operated mice (n = 5) were compared to the scar tissue (n = 8; infarct zone) of mice undergoing MI. Moreover, the gene expression in the non-infarcted area (n = 8; remote zone) of the left ventricle was analyzed as an internal control. Figure 20 shows the expression of cardiovascular candidate genes after MI and Figure 21 presents the expression of homoarginine-dependent candidate genes after MI. Of the twelve validated candidate genes, ten also demonstrated a regulation after MI. These genes included *Hcn2*, *Hcn4*, *Pip5k1b, Scn4a* and *Scn4b* that showed a significant mRNA down-regulation in the infarcted area and *B4galt6*, *Cdkn1a*, *Ctgf*, *Nppa* and *Ucp2* that were up-regulated. No significant difference was overserved for *Ccl11* and *Ccbe1*.
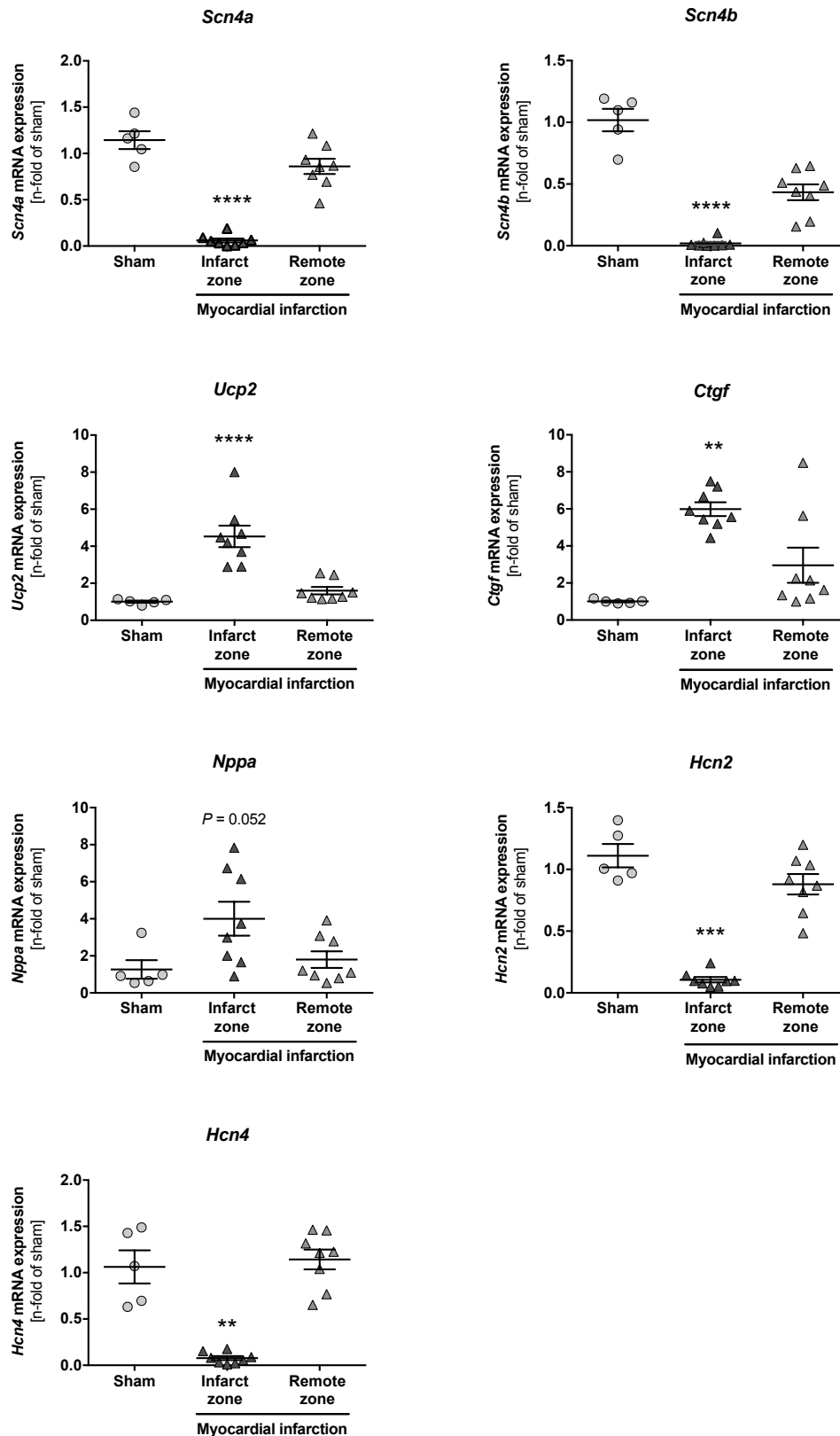
**Figure 20: qPCR expression analysis of cardiovascular candidate genes after myocardial infarction**

The mRNA expression was measured five days after myocardial infarction in left ventricular heart tissue. For analysis C57BL/6J wild-type mice were used. Values are expressed as mean ± SEM. ** $P$ < 0.01; *** $P$ < 0.001 and **** $P$ < 0.0001 versus sham, Kruskal-Wallis-Test. Sham n = 5, myocardial infarction (infarct zone, n = 8), myocardial infarction (remote zone, n = 8).
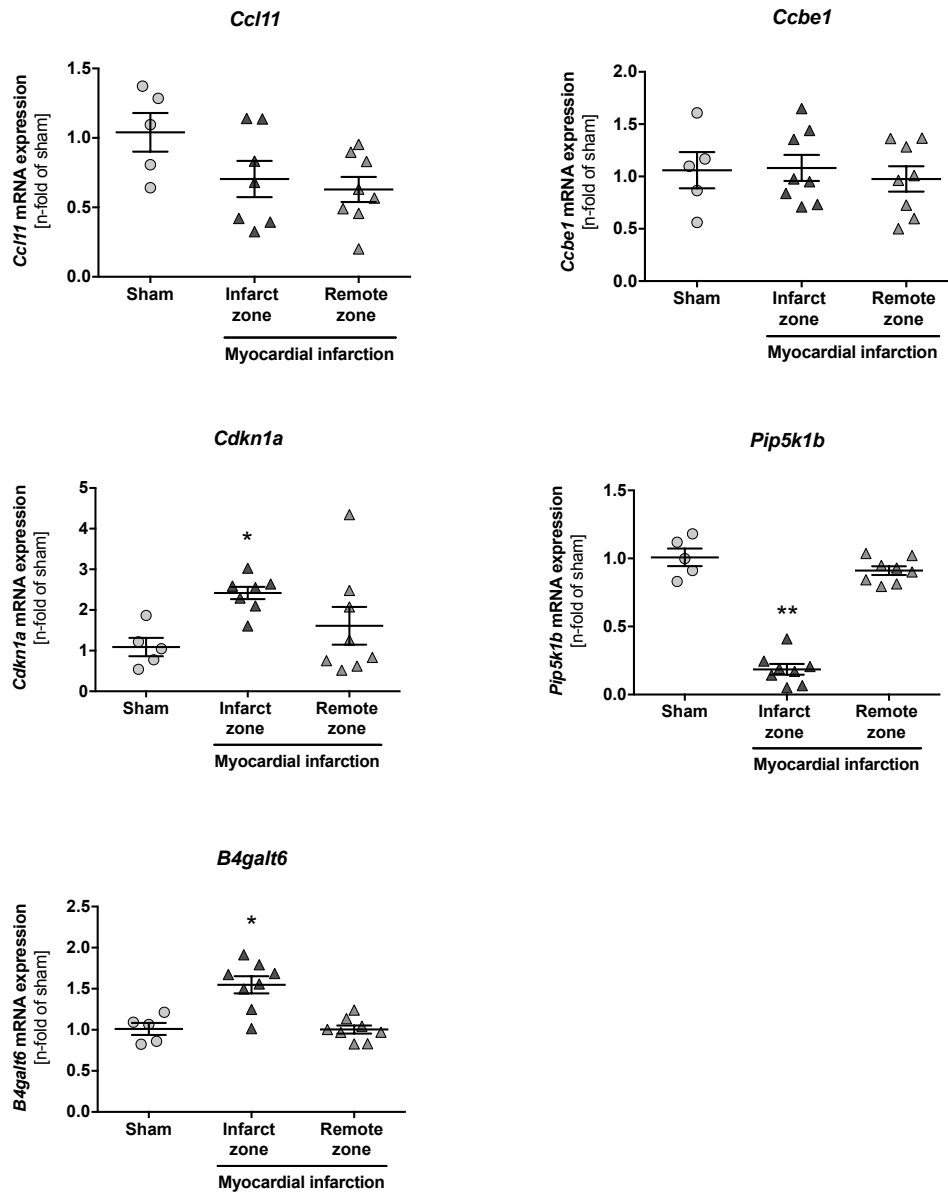
**Figure 21: qPCR expression analysis of homoarginine-dependent candidate genes after myocardial infarction**
The mRNA expression was measured five days after myocardial infarction in left ventricular heart tissue. For analysis C57BL/6J wild-type mice were used. Values are expressed as mean ± SEM. * $P < 0.05$ and ** $P < 0.01$ versus sham, Kruskal-Wallis-Test. Sham n = 5, myocardial infarction (infarct zone, n = 8), myocardial infarction (remote zone, n = 8).

### 5.4.2 *In silico* analysis of candidate genes after myocardial infarction

To validate the results from qPCR analysis and to evaluate the time-dependent regulation of the expression of candidate genes after MI, an *in silico* analysis was performed using GEO expression data (GEO dataset GSE775). The gene expression was analyzed at six time points after experimental induced left coronary artery occlusion. For analysis sham operated mice (n = 4) and mice after MI (n = 3; tissue from the infarcted area) were compared with each other. Differential gene expression was calculated with the GEO2R program and the significance level was set to ≤ 0.05. Figure 22 shows the expression of candidate genes after MI. *B4galt6* mRNA was significantly regulated 24 hours and one week after MI. *Ctgf* and *Pip5k1b* were differentially expressed at all six time points after MI. *Cdkn1a* and *Hcn2* were regulated after four hours and *Nppa* after 24 hours until the last measurements at eight weeks after MI. This indicates that these genes play a role in the acute phase as well as in the transition to the chronic phase in progression to heart failure. Moreover, the analysis revealed a significant up-regulation of *Ccl11* four hours after MI. In this experiment no data were available for the expression of *Ccbe1*, *Hcn4*, *Scn4a*, *Scn4b* and *Ucp2.*
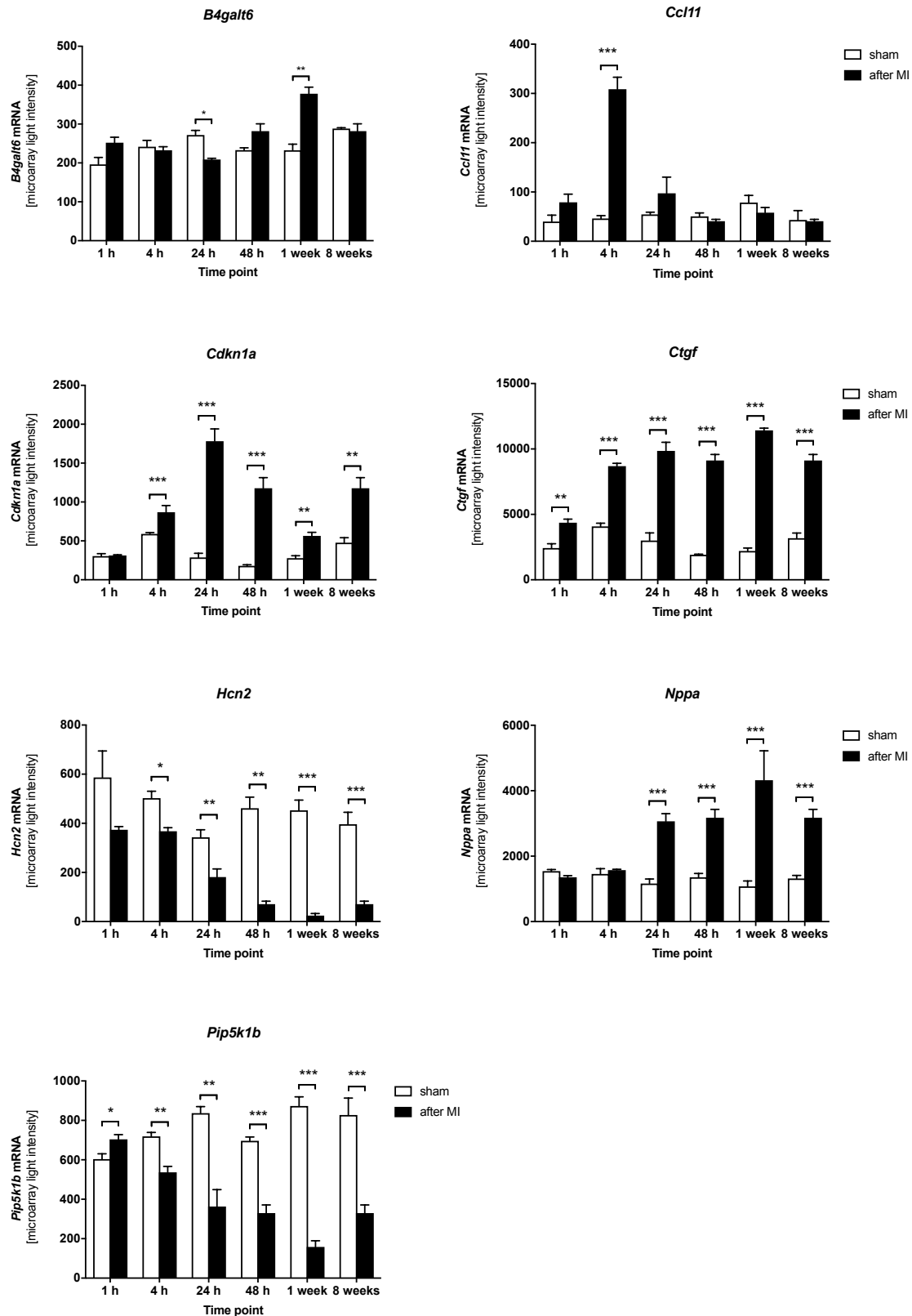
**Figure 22: In silico expression analysis of candidate genes after myocardial infarction**
Relative mRNA expression measured in microarray light intensity at 1 h, 4 h, 24 h, 48 h, 1 week and 8 weeks after experimental induced MI. The GEO dataset GSE775 (Mouse model of myocardial infarction) was used. * $P < 0.05$; ** $P < 0.01$ and *** $P < 0.001$ versus sham. MI: myocardial infarction.

# 6 Discussion

Research on CVD represents a major field of clinical and experimental investigations, nevertheless CVD still remains the leading cause of death in Western countries. To further understand the complex pathophysiological processes and identify novel therapeutic strategies, detailed analysis on underlying genetic and molecular mechanisms are required. In this context, the enzyme AGAT is of strong interest since it is responsible for endogenous homoarginine and creatine formation (Atzler et al., 2015). A lack of creatine results in altered cardiac energy metabolism and low homoarginine plasma levels are associated with poor prognosis in CVD (Lygate et al., 2013b, Atzler et al., 2014). The goal of this work was to gain insights into the molecular signatures linking AGAT, homoarginine and creatine with its implications in CVD. The work focused on detailed investigations on mRNA and miRNA expression level.

## 6.1 Analysis of AGAT-related gene expression in the heart

Lately, it has been shown that AGAT$^{-/-}$ mice exhibit a cardiovascular phenotype of low left ventricular systolic pressure and maximal heart rate in response to dobutamine infusion, with impaired contractility, relaxation and inotropic reserve compared to WT (Faller et al., 2017). Creatine and homoarginine supplementation restored normal hemodynamic parameters partially and completely, respectively. One aim of this work was to answer the question whether differential gene expression in AGAT$^{-/-}$ mice can be linked to the cardiovascular system. Furthermore, a conclusion of whether homoarginine or creatine is the underlying driver of detected changes will be drawn. Given that an impaired AGAT activity contributes to lower homoarginine levels (Choe et al., 2013a, Davids et al., 2012), which in turn predict cardiovascular outcome, examinations on the transcriptome level should help to identify signatures linking AGAT deficiency to susceptibility for cardiovascular events.

### 6.1.1 Influence of AGAT deficiency on gene expression

**AGAT deficiency and molecular pathways**

To evaluate effects of AGAT deficiency itself, differential gene expression analyses were carried out in WT and AGAT$^{-/-}$ mice. In total, the analyses showed 485 significantly regulated genes between both groups (FDR ≤ 0.05). Further characterization by pathway analyses revealed that differentially expressed genes were especially enriched in pathways involved in energy metabolism such as fatty acid biosynthesis, mitochondrial LC-fatty acid beta-oxidation, fatty acid beta-oxidation and glycogen metabolism. The connection of AGAT deficiency and energy metabolism was not surprising, because AGAT deficiency results in diminished intracellular energy stores i.e. ATP and PCr in brain and skeletal muscle (Choe et al., 2013b, Nabuurs et al., 2013). In AGAT$^{-/-}$ hearts, PCr was completely absent, but ATP remained at WT level (Faller et al., 2017). The findings indicate that AGAT$^{-/-}$ mice are able to compensate cardiac ATP levels, which might be reflected by ATP synthesis independent of the creatine/PCr system (e.g. anaerobic glycolysis). Most of above mentioned pathways belong to the lipid metabolism and a compensatory up-regulation of the beta-oxidation might be reasonable. However, further analysis revealed that all lipid-related genes were down-regulated in AGAT$^{-/-}$ mice. Therefore, ongoing research is required to uncover alternative mechanisms of ATP synthesis. Nevertheless, it has to be considered that a compensatory mechanism is assumed in a normally functioning heart. In case of a stressful situation such as MI, heart failure or cardiac arrhythmias, the demand for energy is even higher and the starting conditions in AGAT$^{-/-}$ mice characterized by altered energy metabolism might aggravate the situation.

In addition to demonstrating an association to energy metabolism, pathway analyses revealed a connection to cardiac contractility. Within the top ten pathways, an enrichment of genes in the calcium regulation of the cardiac cells was observed. Calcium is a critical regulator of cardiac myocyte function and represents the link between electrical signals that activate the heart and contraction of myocytes to pump blood (Fearnley et al., 2011). A deregulation of calcium leads to several cardiac dysfunctions, i.e. impaired contractility, relaxation and inotropic reserve. Therefore, the observation provides first

evidence of underlying molecular mechanisms that could explain altered cardiac function in AGAT$^{-/-}$ mice.

**AGAT-related cardiovascular candidate genes**

Another aim was to select candidate genes with a pivotal role regarding cardiovascular changes between WT and AGAT$^{-/-}$ mice. *Scn4a*, *Scn4b*, *Hcn2*, *Hcn4*, *Nppa, Ctgf* and *Ucp2* were identified by network analysis based on a known association to the cardiovascular system and strong connectivity to other genes implying a central regulatory function.

Interestingly, especially genes coding for ion channels appear to be AGAT-dependent. SCN4A, SCN4B, HCN2 and HCN4 belong to this group of membrane proteins. In the heart, ion channels are essential for the cardiac conduction system. More detailed, *Scn4a* and *Scn4b* are coding for voltage-gated sodium channels. The expression of SCN4A in ventricular tissue acts antiarrhythmic and preserves normal conduction in murine hearts after MI (Coronel et al., 2010, Lau et al., 2009). Mutations in *Scn4b* are associated with atrial fibrillation (Li et al., 2013). Both channels are found to be significantly down-regulated within the comparison of WT and AGAT$^{-/-}$ mice. Therefore, the observation that SCN4A acts antiarrhythmic in ventricular tissue might indicate that AGAT$^{-/-}$ mice are more susceptible for arrhythmias, which especially in an injured heart can be of critical importance. *Hcn2* and *Hcn4* are coding for HCN channels and their current plays a key role in the generation and modulation of cardiac rhythmicity (Robinson and Siegelbaum, 2003). HCN4 is highly expressed in the cardiac pace maker region and controls the rhythmic activity of the heart (DiFrancesco, 2010). Compared to HCN4, HCN2 is not that widely expressed in the heart, however, studies revealed that it contributes to spontaneous rhythmic activity (Vaccari et al., 1999). Regarding CVD, several mutations in the *Hcn4* gene have been shown to cause arrhythmias (Baruscotti et al., 2010) and the cardiac-specific knockout of *Hcn4* in mice leads to the development of bradycardia (Baruscotti et al., 2011). In line with those data, AGAT$^{-/-}$ mice with the down-regulated *Hcn4* gene revealed a lower maximal heart rate compared to WT (Faller et al., 2017). Nevertheless, the performed analysis of left ventricular tissue did not comprise the primary pacemaker of the heart (i.e. the sinus node). However, nodal cells are not only expressed in the sinus node, but additionally in

the complete conduction system. This includes the Purkinje fibers explaining the detection of HCN4 in the left ventricle.

Interestingly, the *Nppa* gene was significantly up-regulated in response to the AGAT knockout. The encoded protein atrial natriuretic peptide (ANP) is a molecular marker of hypertrophy and predicts the outcome of CVD (Wang et al., 2004). The up-regulation of *Nppa* indicates that AGAT$^{-/-}$ mice might develop cardiac hypertrophy, however, another study showed that not all molecular markers of hypertrophy were consistently elevated. It has been demonstrated that mRNA expression of brain natriuretic peptide (BNP) and beta myosin heavy chain (β-MHC) were unchanged and mRNA expression of alpha skeletal actin (α-SA) was reduced in AGAT$^{-/-}$ mice (Faller et al., 2017). Therefore, further investigations are needed to evaluate the link between AGAT deficiency and cardiac hypertrophy.

In AGAT$^{-/-}$ mice *Ctgf* mRNA was significantly up-regulated. Studies demonstrated that the expression of CTGF is enhanced in CVD. More detailed, it has been shown that CTGF is up-regulated in cardiac cells after MI, in heart failure and in advanced atherosclerosis (Ohnishi et al., 1998, Ahmed et al., 2004, Oemar et al., 1997). The up-regulation of *Ctgf* mRNA in AGAT$^{-/-}$ mice in combination with the described involvement in CVD gave first evidence that *Ctgf* plays an important role regarding cardiovascular changes in AGAT$^{-/-}$ mice.

*Ucp2,* which was up-regulated in AGAT$^{-/-}$ mice encodes for a member of the family of inner mitochondrial membrane proteins with a carrier function. Studies on the protein UCP2 revealed that it might act as a regulator of lipid metabolism and plays a role in the control of mitochondria-derived reactive oxygen species (ROS) and diabetes (Saleh et al., 2002). Increasing evidence suggests that UCPs could ameliorate myocardial function by reducing mitochondrial ROS generation and cardiomyocyte apoptosis (Akhmedov et al., 2015). It has to be further evaluated whether the up-regulation of *Ucp2* mRNA might be an adaption to higher production of ROS in AGAT$^{-/-}$ mice.

To verify the importance of the described candidate genes in CVD, qPCR and *in silico* analyses in an experimental mouse model of MI were performed. Given that patients with low homoarginine levels and therefore reduced AGAT activity have a worse prognosis and outcome in CVD, it would be of interest to determine whether the regulation of the candidate genes is involved. One week after

induction of MI, *Scn4a*, *Scn4b*, *Hcn2*, *Hcn4*, *Nppa*, *Ctgf* and *Ucp2* were significantly regulated. A deregulation of these genes in AGAT$^{-/-}$ mice combined with the finding that their expression was also influenced by MI *per se* suggests a molecular link between AGAT and MI.

## 6.1.2 Influence of homoarginine and creatine on gene expression

In recent years, especially homoarginine attracted strong interest since studies clearly indicate that serum homoarginine is a biomarker for cardiovascular function and mortality (März et al., 2010, Pilz et al., 2011b, Atzler et al., 2014, Choe et al., 2013a). However, more intriguing is the possibility that homoarginine could have a direct effect on the disease process. Interestingly, homoarginine supplementation attenuated the impaired cardiac function in a mouse model of post-MI heart failure (Atzler et al., 2017). This finding suggests that homoarginine is not only a marker of low creatine stores, but could directly influence cardiovascular function.

To address this question, AGAT$^{-/-}$ mice were supplemented either with homoarginine or creatine and differential gene expression was evaluated between WT and supplemented AGAT$^{-/-}$ mice. A comparison of WT and AGAT$^{-/-}$Cr mice revealed only eight significantly regulated genes (*Agat*, *Mcm8*, *Pde1c*, *Mertk*, *Hmcn1*, *Cds2*, *Rasgef1b*, *Gm14085*) implying that creatine normalizes most of the altered gene expression profile of AGAT$^{-/-}$ mice. The regulation of the cardiovascular candidate genes and previously described pathways is of critical importance for the cardiovascular system. Therefore, analyses whether creatine normalizes their expression were carried out. Of note, both, microarray and qPCR confirmed a normalization of all cardiovascular candidate genes by creatine. The normalization of gene expression by creatine also applies for the energy metabolism. It was not surprising that the change of gene expression regarding this system was mainly creatine-dependent, because creatine plays a key role in buffering chemical energy (ATP) in organs with high energy requirements in form of PCr (Wyss and Kaddurah-Daouk, 2000, Lygate et al., 2013a). Hence, the loss of creatine is responsible for disturbed energy metabolism (Nabuurs et al., 2013). To what extent these changes influence the cardiovascular phenotype in AGAT$^{-/-}$ mice is not fully conclusive yet, but the

observation that creatine supplementation corrected LV systolic pressure might be associated with a normalization of gene expression by creatine.

However, another study analyzing the cardiac phenotype of AGAT^{-/-} mice revealed only a partial rescue of functional parameters by creatine supplementation. Of note, homoarginine supplementation was able to normalize all measured parameters (Faller et al., 2017). So far, at least on gene expression level, a connection could not be established. Neither the expression of cardiovascular candidate genes, nor changes in important molecular pathways were rescued by homoarginine supplementation in AGAT^{-/-} mice. If the positive effect of homoarginine on the phenotype is not explainable by normalization of suggested candidate genes and pathways, a regulation of other genes might occur as consequence of homoarginine supplementation. Therefore, candidate genes were selected, which expression was rescued by homoarginine supplementation in AGAT^{-/-} mice. The basis for this approach was the comparison of genes, which were differentially expressed between WT and AGAT^{-/-} mice as well as between AGAT^{-/-} and AGAT^{-/-}HA mice, but were regulated in the opposite direction. Five genes have been identified (*B4galt6*, *Ccbe1*, *Ccl11*, *Cdkn1a*, *Pip5k1b*), but only *Ccl11* was already described in relation to CVD. This chemokine also known as eosinophil chemotactic protein or eotaxin-1 was implicated in atherosclerosis (Haley et al., 2000, Wang et al., 2013). To evaluate the importance of the other genes in CVD, qPCR and *in silico* analyses in a mouse model of MI were carried out. The results revealed that *B4galt6*, *Cdkn1a* and *Pip5k1b* are regulated after MI. Therefore, further analyses are needed to investigate their exact role. However, the validation of the five genes by qPCR in the AGAT^{-/-} mouse model showed that also creatine leads to an adaption towards the WT.

Although homoarginine supplementation did not normalize the gene expression back to WT, a strong effect of homoarginine itself on the gene expression was identified. 785 genes were differentially expressed between WT and AGAT^{-/-}HA. About half of the regulations can be explained by AGAT deficiency, the rest is attributable to homoarginine only. An explanation for this strong effect might be a supra-physiological homoarginine supplementation.

To conclude, the results on gene expression level revealed that creatine, rather than homoarginine supplementation restored the expression profile in

AGAT$^{-/-}$ towards the WT mice. These findings regarding gene expression level contrast with the observations of Faller et. al., which crucially showed that creatine partly but homoarginine supplementation fully compensated the cardiovascular phenotype in AGAT$^{-/-}$ mice. Thus, further analyses ought to be performed in order to find molecular explanations. One possibility includes changes on protein level, such as post-translational modifications of proteins which then lead to impaired or decreased function.

## 6.2  Analysis of AGAT-related miRNA expression in the heart

Latest research increasingly focused on miRNAs as key regulators of biological processes linked to cardiovascular pathologies (Romaine et al., 2015). In addition, studies reported miRNAs as promising new diagnostic and prognostic biomarkers in the field of CVD (Schulte and Zeller, 2015). So far, miRNAs in the AGAT$^{-/-}$ mouse model have not been evaluated and therefore this was the first approach to gain insight into the complex interaction of mRNAs and miRNAs. The analysis of differential miRNA expression was carried out by miRNA sequencing for the groups of WT, AGAT$^{-/-}$ and AGAT$^{-/-}$HA mice. To validate the results and include the group of creatine-fed mice, qPCR analyses were performed.

### 6.2.1  Influence of AGAT deficiency on miRNA expression

The first comparison of WT and AGAT$^{-/-}$ mice showed 30 significantly regulated miRNAs between the groups. Literature-based research revealed that nine of them were already linked to cardiovascular pathologies.
The sequencing showed that among the nine cardiovascular candidate miRNAs, miR-30b, miR-30d, miR-125b, miR-130a, miR-210, miR-181c and let-7i were up-regulated and miR-100 as well as miR-204 were down-regulated in AGAT$^{-/-}$ left ventricular heart tissue. With regard to the cardiovascular system, it has been suggested that miR-30b is involved in cardiac hypertrophy (He et al., 2013), whereas miR-30d and miR-181c were linked to heart failure (Das et al., 2014, Melman et al., 2015). Interestingly, miR-100 plays a role in cardiovascular homeostasis by regulating natriuretic peptides, including ANP (Wong et al., 2015). ANP is encoded by the *Nppa* gene and a deregulation of this gene has been observed in the transcriptome analysis. Therefore, the possibility of a

connection between both findings is given and needs further investigations. An association with cardiac arrhythmias (Osbourne et al., 2014) and proliferation of smooth muscle cells in hypertension (Wu et al., 2011) was shown for miR-130a. miR-210 is linked to the hypoxia pathway (Han et al., 2011) and overexpressed in cells affected by CVD (Mutharasan et al., 2011). Finally, the let-7 family including let-7i was found to be highly expressed in the cardiovascular system and involved in CVD, such as dilated cardiomyopathy (Satoh et al., 2011, Bao et al., 2013). A deregulation of these miRNAs in AGAT$^{-/-}$ mice from the beginning might aggravate the physiological situation in case of a cardiovascular event.

Moreover, the differential expression of specific miRNAs might influence cardiovascular risk factors. Interestingly, miR-125b and miR-204 might lead to the calcification of smooth muscle cells (Cui et al., 2012, Goettsch et al., 2011). As is commonly known, atherosclerosis is a risk factor for CVD and it is possible that AGAT$^{-/-}$ mice are more susceptible for the development of calcifications. Further investigations might include histological and functional investigations of the aorta and coronary arteries. Moreover, the connection to atherosclerosis and vascular function is of particular interest since homoarginine is involved in NO metabolism, which plays an important role in vascular function and oxidative stress.

### 6.2.2 Influence of homoarginine and creatine on miRNA expression

The analysis of homoarginine-dependent effects on cardiac miRNA expression showed 46 significantly regulated miRNAs between WT and AGAT$^{-/-}$HA mice. Of the 30 regulated miRNAs between WT and AGAT$^{-/-}$ mice, eight did not remain differentially expressed between WT and AGAT$^{-/-}$HA mice. Interestingly, these eight miRNAs included the cardiovascular candidate miRNAs miR-181c and let-7i. Further investigations are needed to evaluate the role of homoarginine-dependent miRNAs, especially miR-181c and let-7i, in relation to altered cardiac function in AGAT$^{-/-}$ mice.

The higher number of regulated miRNAs suggests that, besides the influence of AGAT deficiency, an effect of homoarginine alone exists. As mentioned previously, an explanation might be the supra-physiological supplementation of homoarginine. Within the comparison of WT versus AGAT$^{-/-}$HA and AGAT$^{-/-}$

versus AGAT$^{-/-}$HA, especially miR-301b, miR-378b and miR-3969 seem to be homoarginine-dependent. More detailed, miR-378b showed an up-regulation and miR-301b as well as miR-3969 a strong down-regulation in the AGAT$^{-/-}$HA group. The cardiovascular molecular impact of these miRNAs has to be further evaluated but first studies revealed that miR-301b was up-regulated in patients with atrial fibrillation (Wang et al., 2012).

The validation of the candidate miRNAs by qPCR, which also included the group of AGAT$^{-/-}$Cr mice, showed the tendency that the expression of miR-30d, miR-130a and miR-204 was rescued in AGAT$^{-/-}$Cr mice.

In contrast to the extent of gene expression, more than half of observed differentially expressed miRNAs showed a regulation less than 50%. Given that one miRNA can regulate the expression of several mRNAs (Mohr and Mott, 2015), even a small change in expression can lead to complex biological changes. However, the small changes were challenging in the qPCR analysis and could not be detected as precisely as via miRNA sequencing. This might be attributable to the small number of biological replicates (4-7 per group) and technical variations that lead to Ct value changes and interfere with the small FC.

## 6.3   Regulatory mechanisms within the AGAT metabolism

The study gave first evidence that differentially expressed miRNAs might modulate the expression of significantly regulated mRNAs within the AGAT metabolism. Between WT and AGAT$^{-/-}$ mice, 30 differentially expressed miRNAs were discovered. Here, nine miRNAs with known association to the cardiovascular system were selected as candidates. Looking-up predicted binding sites of miRNAs in publicly available online databases showed that groups of differentially expressed genes might be regulated by one of the selected miRNAs. Interestingly, the candidate genes *B4galt6*, *Scn4a*, *Scn4b* and *Ucp2* were predicted to be regulated by the cardiovascular candidate miRNAs miR-30b, miR-30d, miR-125b, miR-210 and let-7i. Besides *Ucp2* and miR-210, which interaction was experimental validated, other interactions are only predicted *in silico* via bioinformatics analysis. In order to verify the predicted interaction, experiments that investigate the mRNA expression by up- or down-

regulation of miRNA activity using either miRNA mimics or inhibitors ought to be performed.

## 6.4 Limitations

For mRNA and miRNA analysis, only left ventricular heart tissue was used. Therefore, not all transcriptome changes were detected, which determine the cardiac phenotype of AGAT$^{-/-}$ mice. In particular, AGAT$^{-/-}$ mice revealed a reduced heart rate compared to WT mice (Faller et al., 2017). Therefore, detailed investigations of the cardiac conduction system, i.e. especially sinus node and atrioventricular node, seem reasonable. Both are located in the right atrium, which was not analyzed in this study. Moreover, an involvement of homoarginine and thus AGAT in the L-arginine and NO metabolism was assumed. Homoarginine inhibits arginase and therefore increases L-arginine availability and facilitates NO production (Hrabak et al., 1994). Furthermore, homoarginine itself can serve as a substrate for NO synthesis. Since NO acts as a vasodilator in coronary arteries, analysis of gene expression in the vessels constitutes another starting point.

Although transcriptome analysis can be used to identify differential gene expression, the influence on the organism is mainly conducted by resulting changes on protein expression level. The translation of the findings from gene to protein expression level represents a critical point in research, especially when using high-throughput methods. In this study, the validation by qPCR confirmed all candidate genes, the validation on protein expression level was not successful. On the one hand, finding a working antibody was technically challenging. On the other hand, the low expression of HCN2 and HCN4 in relation to the whole left ventricle might be an explanation for the difficulties that occurred. Another explanation why ANP protein could not be detected might be the fact that although it is transcribed and translated in the heart, it is mostly secreted into the blood.

## 6.5  Outlook

This study provided first insights into the molecular background of the AGAT metabolism and the influence of homoarginine and creatine on molecular pathways. However, the question through which mechanisms homoarginine acts protectively in the cardiovascular system and is able to normalize the cardiovascular phenotype of AGAT$^{-/-}$ mice still needs to be answered. Since the gene expression analysis did not lead to an explanation, further investigations ought to be performed. For instance, by performing metabolome and proteome analyses, the systems biology approach can be completed. Moreover, post-translational modifications should be considered to explain the cardiac phenotype of AGAT$^{-/-}$ mice.

# 7 Summary

AGAT is the responsible enzyme for the formation of the cardiovascular risk marker homoarginine. Moreover, AGAT catalyzes the first and rate-limiting step of creatine synthesis, which is essential for cardiac energy metabolism. AGAT$^{-/-}$ mice exhibit a cardiac dysfunction, which was corrected in part by creatine and totally by homoarginine supplementation. So far, data on the underlying transduction pathways are scant.

The aim of the present study was to gain insights into the molecular signatures on mRNA and miRNA level linking AGAT, homoarginine and creatine deficiency with CVD. Comprehensive investigations in an AGAT$^{-/-}$ mouse model delivered information about AGAT-related molecular changes. On the gene expression level, the results reveal that AGAT deficiency led to significant differential gene expression, mainly influencing cardiac energy metabolism and contractility pathways. In addition, candidate genes were identified in AGAT$^{-/-}$ mice, which can be linked to cardiovascular changes. Basis for this was a known association to CVD (*Scn4a*, *Scn4b*, *Hcn2*, *Hcn4*, *Ctgf*, *Nppa*, *Ucp2*) or restored gene expression by homoarginine (*Ccl11*, *Ccbe1*, *Cdkn1a*, *Pip5k1b*, *B4galt6*). The importance of these genes regarding CVD could be confirmed in an experimental MI mouse model, *in silico* and *in vivo*. On miRNA expression level, differentially expressed miRNAs between WT and AGAT$^{-/-}$ mice with a role in the cardiovascular system were identified (miR-30b, miR-30d, miR-125b, miR-210, let-7i), which might also influence the expression of regulated candidate genes (*B4galt6*, *Scn4a*, *Scn4b*, *Ucp2*).

Studies on AGAT$^{-/-}$ mice demonstrated a normalization of cardiac parameters by homoarginine and not creatine. However, on gene expression level, creatine, but not homoarginine, was able to rescue the expression towards the WT. Therefore, the question why homoarginine leads to a normalization of the cardiovascular phenotype still remains to be answered. Apart from changes in the gene expression or associated miRNA regulations, the positive effects of homoarginine might be found elsewhere, such as in direct interactions with proteins thereby regulating their function.

# 8 Zusammenfassung

Das Enzym AGAT ist für die Synthese des kardiovaskulären Risikomarkers Homoarginin verantwortlich. Darüber hinaus ist AGAT an der Bildung von Kreatin beteiligt, das für den kardialen Energiestoffwechsel von großer Bedeutung ist. AGAT$^{-/-}$ Mäuse zeigen einen veränderten kardiovaskulären Phänotyp, welcher teilweise durch Kreatin und vollständig durch Homoarginin normalisiert werden konnte. Die zugrundeliegenden molekularen Mechanismen sind bislang nicht bekannt.

Ziel dieser Arbeit war es, die AGAT-abhängigen molekularen Veränderungen auf mRNA- und miRNA-Ebene und deren Einfluss auf das kardiovaskuläre System zu evaluieren. Dafür wurden umfassende Untersuchungen in einem AGAT$^{-/-}$ Mausmodell durchgeführt. Auf mRNA-Ebene konnte gezeigt werden, dass AGAT-Mangel zu einer signifikant veränderten Genexpression führt, welche insbesondere molekulare Pathways des kardialen Energiestoffwechsels als auch der Kontraktilität des Herzmuskels betrifft. Zudem konnten kardiovaskuläre Kandidaten-Gene in AGAT$^{-/-}$ Mäusen identifiziert werden. Grundlage hierfür war eine bekannte Assoziation zum Herz-Kreislauf-System (*Scn4a*, *Scn4b*, *Hcn2*, *Hcn4*, *Ctgf*, *Nppa*, *Ucp2*) oder eine normalisierte Genexpression durch Homoarginin (*Ccl11*, *Ccbe1*, *Cdkn1a*, *Pip5k1b*, *B4galt6*). *In silico* und *in vivo* Analysen in einem MI-Mausmodell konnten bestätigen, dass diese Gene eine wichtige Rolle in kardiovaskulären Erkrankungen spielen. Auf miRNA-Ebene wurden potentielle regulatorische Einflüsse auf die Genexpression untersucht. Es zeigten sich differentiell exprimierte miRNAs zwischen WT und AGAT$^{-/-}$ Mäusen, welche in der Literatur bereits im Rahmen kardiovaskulärer Pathologien beschrieben wurden (miR-30b, miR-30d, miR-125b, miR-210, let-7i). Interessanterweise scheinen diese miRNAs auch einige der zuvor identifizierten Kandidaten-Gene (*B4galt6*, *Scn4a*, *Scn4b*, *Ucp2*) zu regulieren.

Die Studien an AGAT$^{-/-}$ Mäusen zeigten eine vollständige Normalisierung der Herzfunktion durch Homoarginin. Auf Genexpressions-Ebene konnte jedoch Kreatin, nicht Homoarginin, die Expression in Richtung WT angleichen. Die Frage, warum Homoarginin zu einer Normalisierung des kardiovaskulären

Phänotyps führt, bleibt daher weiterhin offen. Abgesehen von Veränderungen auf RNA-Ebene, könnte Homoarginin auch durch direkte Protein-Interaktion Einfluss auf das kardiovaskuläre System nehmen.

# 9 List of abbreviations

| | |
|---|---|
| °C | Degree Celsius |
| ADP | Adenosine diphosphate |
| AGAT | L-arginine:glycine amidinotransferase |
| ANP | Atrial natriuretic peptide |
| APS | Ammonium persulfate |
| ATP | Adenosine triphosphate |
| B4GALT6 | Beta-1,4-galactosyltransferase 6 |
| BCA | Bicinchoninic acid |
| BSA | Bovine serum albumin |
| CAD | Coronary artery disease |
| CCBE1 | Collagen and calcium binding EGF domains 1 |
| CCL11 | C-C motif chemokine ligand 1 |
| CDKN1A | Cyclin dependent kinase inhibitor 1A |
| cDNA | Complementary deoxyribonucleic acid |
| CK | Creatine kinase |
| Cr | Creatine |
| cRNA | Complementary ribonucleic acid |
| Ct | Cycle threshold |
| CTGF | Connective tissue growth factor |
| Cu | Cuprum |
| CVD | Cardiovascular disease |
| DNA | Deoxyribonucleic acid |
| dNTP | Deoxynucleotide |
| $dp/dt_{max}$ | Rate of pressure rise maximum |
| $dp/dt_{min}$ | Rate of pressure rise minimum |
| EC | Enzyme Commission |
| EDTA | Ethylenediaminetetraacetic acid electrophoresis |
| et al. | et alteri |
| FC | Fold change |
| FDR | False discovery rate |
| g | Gram |
| GAA | Guanidinoacetic acid |
| GAMT | Guanidinoacetate N-methyltransferase |
| GEO | Gene Expression Omnibus |
| GWAS | Genome-wide association study |
| h | Hour |

| | |
|---|---|
| HA | Homoarginine |
| HCN2 | Hyperpolarization-activated cyclic nucleotide-gated ion channel 2 |
| HCN4 | Hyperpolarization-activated cyclic nucleotide-gated ion channel 4 |
| i.e. | id est |
| Ig | Immunoglobulin |
| l | Liter |
| LV | Left ventricular |
| mg | Milligram |
| MI | Myocardial infarction |
| min | Minute |
| miRNA | Micro ribonucleic acid |
| ml | Milliliter |
| mM | Mmol/liter |
| mmol | Millimol |
| mRNA | Messenger ribonucleic acid |
| n | Number |
| NaCl | Sodium chloride |
| NC | Nitrocellulose |
| Neo | Neomycin resistance gene |
| ng | Nanogram |
| NIHSS | National Institutes of Health Stroke Scale |
| nm | Nanometer |
| NO | Nitric oxide |
| NOS | Nitric oxide synthase |
| ns | Not significant |
| NT-proBNP | N-terminal prohormone of brain natriuretic peptide |
| NYHA | New York Heart Association |
| PBS | Phosphate buffered saline |
| PC | Principle component |
| PCA | Principle component analysis |
| PCr | Phosphocreatine |
| PCR | Polymerase chain reaction |
| PIP5K1B | Phosphatidylinositol-4-phosphate 5-kinase type 1 beta |
| qPCR | Quantitative polymerase chain reaction |
| RIN | RNA integrity number |
| RNA | Ribonucleic acid |
| ROS | Reactive oxygen species |
| Rpm | Rounds per minute |
| RT | Reverse transcriptase |
| SCN4A | Sodium voltage-gated channel alpha subunit 4 |

| | |
|---|---|
| SCN4B | Sodium voltage-gated channel beta subunit 4 |
| SDS | Sodium dodecyl sulfate |
| SDS-Page | sodium dodecyl sulfate polyacrylamide gel |
| sec | Second |
| SEM | Standard error of the mean |
| TBS | Tris-buffered saline |
| TBS-T | Tris-buffered saline with Tween 20 |
| TEMED | N,N,N',N'-Tetramethylethylenediamine |
| U | Unit |
| UCP2 | Uncoupling protein 2 |
| V | Volt |
| WGCNA | Weighted correlation network analysis |
| WT | Wild-type |
| µg | Microgram |
| µl | Microliter |

# 10 Bibliography

AHMED, M. S., OIE, E., VINGE, L. E., YNDESTAD, A., OYSTEIN ANDERSEN, G., ANDERSSON, Y., ATTRAMADAL, T. & ATTRAMADAL, H. 2004. Connective tissue growth factor--a novel mediator of angiotensin II-stimulated cardiac fibroblast activation in heart failure in rats. *J Mol Cell Cardiol,* 36**,** 393-404.

AKHMEDOV, A. T., RYBIN, V. & MARIN-GARCIA, J. 2015. Mitochondrial oxidative metabolism and uncoupling proteins in the failing heart. *Heart Fail Rev,* 20**,** 227-49.

ANDERS, S. & HUBER, W. 2010. Differential expression analysis for sequence count data. *Genome Biol,* 11**,** R106.

ATZLER, D., BAUM, C., OJEDA, F., KELLER, T., CORDTS, K., SCHNABEL, R. B., CHOE, C. U., LACKNER, K. J., MUNZEL, T., BOGER, R. H., BLANKENBERG, S., SCHWEDHELM, E. & ZELLER, T. 2016. Low Homoarginine Levels in the Prognosis of Patients With Acute Chest Pain. *J Am Heart Assoc,* 5**,** e002565.

ATZLER, D., GORE, M. O., AYERS, C. R., CHOE, C. U., BOGER, R. H., DE LEMOS, J. A., MCGUIRE, D. K. & SCHWEDHELM, E. 2014. Homoarginine and cardiovascular outcome in the population-based Dallas Heart Study. *Arterioscler Thromb Vasc Biol,* 34**,** 2501-7.

ATZLER, D., MCANDREW, D. J., CORDTS, K., SCHNEIDER, J. E., ZERVOU, S., SCHWEDHELM, E., NEUBAUER, S. & LYGATE, C. A. 2017. Dietary Supplementation with Homoarginine Preserves Cardiac Function in a Murine Model of Post-Myocardial Infarction Heart Failure. *Circulation,* 135**,** 400-402.

ATZLER, D., ROSENBERG, M., ANDERSSOHN, M., CHOE, C. U., LUTZ, M., ZUGCK, C., BOGER, R. H., FREY, N. & SCHWEDHELM, E. 2013. Homoarginine--an independent marker of mortality in heart failure. *Int J Cardiol,* 168**,** 4907-9.

ATZLER, D., SCHWEDHELM, E. & CHOE, C. U. 2015. L-homoarginine and cardiovascular disease. *Curr Opin Clin Nutr Metab Care,* 18**,** 83-8.

BAO, M. H., FENG, X., ZHANG, Y. W., LOU, X. Y., CHENG, Y. & ZHOU, H. H. 2013. Let-7 in cardiovascular diseases, heart development and cardiovascular differentiation from stem cells. *Int J Mol Sci,* 14**,** 23086-102.

BARUSCOTTI, M., BOTTELLI, G., MILANESI, R., DIFRANCESCO, J. C. & DIFRANCESCO, D. 2010. HCN-related channelopathies. *Pflugers Arch,* 460**,** 405-15.

BARUSCOTTI, M., BUCCHI, A., VISCOMI, C., MANDELLI, G., CONSALEZ, G., GNECCHI-RUSCONI, T., MONTANO, N., CASALI, K. R., MICHELONI, S., BARBUTI, A. & DIFRANCESCO, D. 2011. Deep bradycardia and heart block caused by inducible cardiac-specific knockout of the pacemaker channel gene Hcn4. *Proc Natl Acad Sci U S A,* 108**,** 1705-10.

BRAISSANT, O. & HENRY, H. 2008. AGAT, GAMT and SLC6A8 distribution in the central nervous system, in relation to creatine deficiency syndromes: a review. *J Inherit Metab Dis,* 31**,** 230-9.

BROWN, G. R., HEM, V., KATZ, K. S., OVETSKY, M., WALLIN, C., ERMOLAEVA, O., TOLSTOY, I., TATUSOVA, T., PRUITT, K. D., MAGLOTT, D. R. & MURPHY, T. D. 2015. Gene: a gene-centered information resource at NCBI. *Nucleic Acids Res,* 43**,** D36-42.

CHOE, C.-U., SCHWEDHELM, E. & ATZLER, D. 2017. Homoarginine and l-Arginine/Glycine Amidinotransferase in Stroke. *In:* PATEL, V. B., PREEDY, V. R. & RAJENDRAM, R. (eds.) *L-Arginine in Clinical Nutrition.* Cham: Springer International Publishing.

CHOE, C. U., ATZLER, D., WILD, P. S., CARTER, A. M., BOGER, R. H., OJEDA, F., SIMOVA, O., STOCKEBRAND, M., LACKNER, K., NABUURS, C., MARESCAU, B., STREICHERT, T., MULLER, C., LUNEBURG, N., DE DEYN, P. P., BENNDORF, R. A., BALDUS, S., GERLOFF, C., BLANKENBERG, S., HEERSCHAP, A., GRANT, P. J., MAGNUS, T., ZELLER, T., ISBRANDT, D. & SCHWEDHELM, E. 2013a. Homoarginine levels are regulated by L-arginine:glycine amidinotransferase and affect stroke outcome: results from human and murine studies. *Circulation,* 128**,** 1451-61.

CHOE, C. U., NABUURS, C., STOCKEBRAND, M. C., NEU, A., NUNES, P., MORELLINI, F., SAUTER, K., SCHILLEMEIT, S., HERMANS-BORGMEYER, I., MARESCAU, B., HEERSCHAP, A. & ISBRANDT, D. 2013b. L-arginine:glycine amidinotransferase deficiency protects from metabolic syndrome. *Hum Mol Genet,* 22**,** 110-23.

CHOMCZYNSKI, P. & SACCHI, N. 1987. Single-step method of RNA isolation by acid guanidinium thiocyanate-phenol-chloroform extraction. *Anal Biochem,* 162**,** 156-9.

CORONEL, R., LAU, D. H., SOSUNOV, E. A., JANSE, M. J., DANILO, P., JR., ANYUKHOVSKY, E. P., WILMS-SCHOPMAN, F. J., OPTHOF, T., SHLAPAKOVA, I. N., OZGEN, N., PRESTIA, K., KRYUKOVA, Y., COHEN, I. S., ROBINSON, R. B. & ROSEN, M. R. 2010. Cardiac expression of skeletal muscle sodium channels increases longitudinal conduction velocity in the canine 1-week myocardial infarction. *Heart Rhythm,* 7**,** 1104-10.

CUI, R. R., LI, S. J., LIU, L. J., YI, L., LIANG, Q. H., ZHU, X., LIU, G. Y., LIU, Y., WU, S. S., LIAO, X. B., YUAN, L. Q., MAO, D. A. & LIAO, E. Y. 2012. MicroRNA-204 regulates vascular smooth muscle cell calcification in vitro and in vivo. *Cardiovasc Res,* 96**,** 320-9.

CULLEN, M. E., YUEN, A. H., FELKIN, L. E., SMOLENSKI, R. T., HALL, J. L., GRINDLE, S., MILLER, L. W., BIRKS, E. J., YACOUB, M. H. & BARTON, P. J. 2006. Myocardial expression of the arginine:glycine amidinotransferase gene is elevated in heart failure and normalized after recovery: potential implications for local creatine synthesis. *Circulation,* 114**,** I16-20.

DAS, S., BEDJA, D., CAMPBELL, N., DUNKERLY, B., CHENNA, V., MAITRA, A. & STEENBERGEN, C. 2014. miR-181c regulates the mitochondrial genome, bioenergetics, and propensity for heart failure in vivo. *PLoS One,* 9**,** e96820.

DAVIDS, M., NDIKA, J. D., SALOMONS, G. S., BLOM, H. J. & TEERLINK, T. 2012. Promiscuous activity of arginine:glycine amidinotransferase is responsible for the synthesis of the novel cardiovascular risk factor homoarginine. *FEBS Lett,* 586**,** 3653-7.

DIFRANCESCO, D. 2010. The role of the funny current in pacemaker activity. *Circ Res,* 106**,** 434-46.

DRECHSLER, C., MEINITZER, A., PILZ, S., KRANE, V., TOMASCHITZ, A., RITZ, E., MARZ, W. & WANNER, C. 2011. Homoarginine, heart failure, and sudden cardiac death in haemodialysis patients. *Eur J Heart Fail,* 13**,** 852-9.

FALLER, K. M. E., ATZLER, D., MCANDREW, D. J., ZERVOU, S., WHITTINGTON, H. J., SIMON, J. N., AKSENTIJEVIC, D., HOVE, M. T., CHOE, C. U., ISBRANDT, D., CASADEI, B., SCHNEIDER, J. E., NEUBAUER, S. & LYGATE, C. A. 2017. Impaired cardiac contractile function in AGAT knockout mice devoid of creatine is rescued by homoarginine but not creatine. *Cardiovasc Res.*

FEARNLEY, C. J., RODERICK, H. L. & BOOTMAN, M. D. 2011. Calcium signaling in cardiac myocytes. *Cold Spring Harb Perspect Biol,* 3**,** a004242.

GOETTSCH, C., RAUNER, M., PACYNA, N., HEMPEL, U., BORNSTEIN, S. R. & HOFBAUER, L. C. 2011. miR-125b regulates calcification of vascular smooth muscle cells. *Am J Pathol,* 179**,** 1594-600.

GORE, M. O., LUNEBURG, N., SCHWEDHELM, E., AYERS, C. R., ANDERSSOHN, M., KHERA, A., ATZLER, D., DE LEMOS, J. A., GRANT, P. J., MCGUIRE, D. K. & BOGER, R. H. 2013. Symmetrical dimethylarginine predicts mortality in the general population: observations from the Dallas heart study. *Arterioscler Thromb Vasc Biol,* 33**,** 2682-8.

GUTHMILLER, P., VAN PILSUM, J. F., BOEN, J. R. & MCGUIRE, D. M. 1994. Cloning and sequencing of rat kidney L-arginine:glycine amidinotransferase. Studies on the mechanism of regulation by growth hormone and creatine. *J Biol Chem,* 269**,** 17556-60.

HALEY, K. J., LILLY, C. M., YANG, J. H., FENG, Y., KENNEDY, S. P., TURI, T. G., THOMPSON, J. F., SUKHOVA, G. H., LIBBY, P. & LEE, R. T. 2000. Overexpression of eotaxin and the CCR3 receptor in human atherosclerosis: using genomic technology to identify a potential novel pathway of vascular inflammation. *Circulation,* 102**,** 2185-9.

HAN, M., TOLI, J. & ABDELLATIF, M. 2011. MicroRNAs in the cardiovascular system. *Curr Opin Cardiol,* 26**,** 181-9.

HANSSON, G. K. 2005. Inflammation, atherosclerosis, and coronary artery disease. *N Engl J Med,* 352**,** 1685-95.

HE, J., JIANG, S., LI, F. L., ZHAO, X. J., CHU, E. F., SUN, M. N., CHEN, M. Z. & LI, H. 2013. MicroRNA-30b-5p is involved in the regulation of cardiac hypertrophy by targeting CaMKIIdelta. *J Investig Med,* 61**,** 604-12.

HRABAK, A., BAJOR, T. & TEMESI, A. 1994. Comparison of substrate and inhibitor specificity of arginase and nitric oxide (NO) synthase for arginine analogues and related compounds in murine and rat macrophages. *Biochem Biophys Res Commun,* 198**,** 206-12.

HUMM, A., HUBER, R. & MANN, K. 1994. The amino acid sequences of human and pig L-arginine:glycine amidinotransferase. *FEBS Lett,* 339**,** 101-7.

ILLUMINA. 2010. *Illumina Sequencing Technology* [Online]. Available: https://www.illumina.com/documents/products/techspotlights/techspotlight_sequencing.pdf [Accessed 10.12.2017, 10:00].

ITEM, C. B., STOCKLER-IPSIROGLU, S., STROMBERGER, C., MUHL, A., ALESSANDRI, M. G., BIANCHI, M. C., TOSETTI, M., FORNAI, F. & CIONI, G. 2001. Arginine:glycine amidinotransferase deficiency: the third inborn error of creatine metabolism in humans. *Am J Hum Genet,* 69**,** 1127-33.

JAZWINSKA-KOZUBA, A., MARTENS-LOBENHOFFER, J., KRUSZELNICKA, O., RYCAJ, J., CHYRCHEL, B., SURDACKI, A. & BODE-BOGER, S. M. 2013. Opposite associations of plasma homoarginine and ornithine with arginine in healthy children and adolescents. *Int J Mol Sci,* 14**,** 21819-32.

KLEBER, M. E., SEPPALA, I., PILZ, S., HOFFMANN, M. M., TOMASCHITZ, A., OKSALA, N., RAITOHARJU, E., LYYTIKAINEN, L. P., MAKELA, K. M., LAAKSONEN, R., KAHONEN, M., RAITAKARI, O. T., HUANG, J., KIENREICH, K., FAHRLEITNER-PAMMER, A., DRECHSLER, C., KRANE, V., BOEHM, B. O., KOENIG, W., WANNER, C., LEHTIMAKI, T., MARZ, W. & MEINITZER, A. 2013. Genome-wide association study identifies 3 genomic loci significantly associated with serum levels of homoarginine: the AtheroRemo Consortium. *Circ Cardiovasc Genet,* 6**,** 505-13.

KRISKO, I. & WALKER, J. B. 1966. Influence of sex hormones on amidinotransferase levels. Metabolic control of creatine biosynthesis. *Acta Endocrinol (Copenh),* 53**,** 655-62.

LANGFELDER, P. & HORVATH, S. 2008. WGCNA: an R package for weighted correlation network analysis. *BMC Bioinformatics,* 9**,** 559.

LAU, D. H., CLAUSEN, C., SOSUNOV, E. A., SHLAPAKOVA, I. N., ANYUKHOVSKY, E. P., DANILO, P., JR., ROSEN, T. S., KELLY, C., DUFFY, H. S., SZABOLCS, M. J., CHEN, M., ROBINSON, R. B., LU, J., KUMARI, S., COHEN, I. S. & ROSEN, M. R. 2009. Epicardial border zone overexpression of skeletal muscle sodium channel SkM1 normalizes activation, preserves conduction, and suppresses ventricular arrhythmia: an in silico, in vivo, in vitro study. *Circulation,* 119**,** 19-27.

LEWIS, G. D., ASNANI, A. & GERSZTEN, R. E. 2008. Application of metabolomics to cardiovascular biomarker and pathway discovery. *J Am Coll Cardiol,* 52**,** 117-23.

LI, R. G., WANG, Q., XU, Y. J., ZHANG, M., QU, X. K., LIU, X., FANG, W. Y. & YANG, Y. Q. 2013. Mutations of the SCN4B-encoded sodium channel beta4 subunit in familial atrial fibrillation. *Int J Mol Med,* 32**,** 144-50.

LIN, C. W. & FISHMAN, W. H. 1972. L-Homoarginine. An organ-specific, uncompetitive inhibitor of human liver and bone alkaline phosphohydrolases. *J Biol Chem,* 247**,** 3082-7.

LIVAK, K. J. & SCHMITTGEN, T. D. 2001. Analysis of relative gene expression data using real-time quantitative PCR and the 2(-Delta Delta C(T)) Method. *Methods,* 25**,** 402-8.

LLOYD-JONES, D. M. 2010. Cardiovascular risk prediction: basic concepts, current status, and future directions. *Circulation,* 121**,** 1768-77.

LYGATE, C. A., AKSENTIJEVIC, D., DAWSON, D., TEN HOVE, M., PHILLIPS, D., DE BONO, J. P., MEDWAY, D. J., SEBAG-MONTEFIORE, L., HUNYOR, I., CHANNON, K. M., CLARKE, K., ZERVOU, S., WATKINS, H., BALABAN, R. S. & NEUBAUER, S. 2013a. Living without creatine: unchanged exercise capacity and response to chronic myocardial infarction in creatine-deficient mice. *Circ Res,* 112**,** 945-55.

LYGATE, C. A., FISCHER, A., SEBAG-MONTEFIORE, L., WALLIS, J., TEN HOVE, M. & NEUBAUER, S. 2007. The creatine kinase energy transport system in the failing mouse heart. *J Mol Cell Cardiol,* 42**,** 1129-36.

LYGATE, C. A., SCHNEIDER, J. E. & NEUBAUER, S. 2013b. Investigating cardiac energetics in heart failure. *Exp Physiol,* 98**,** 601-5.

MÄRZ, W., MEINITZER, A., DRECHSLER, C., PILZ, S., KRANE, V., KLEBER, M. E., FISCHER, J., WINKELMANN, B. R., BOHM, B. O., RITZ, E. & WANNER, C. 2010. Homoarginine, cardiovascular risk, and mortality. *Circulation,* 122**,** 967-75.

MCGUIRE, D. M., GROSS, M. D., VAN PILSUM, J. F. & TOWLE, H. C. 1984. Repression of rat kidney L-arginine:glycine amidinotransferase synthesis by creatine at a pretranslational level. *J Biol Chem,* 259**,** 12034-8.

MEDEIROS-DOMINGO, A., KAKU, T., TESTER, D. J., ITURRALDE-TORRES, P., ITTY, A., YE, B., VALDIVIA, C., UEDA, K., CANIZALES-QUINTEROS, S., TUSIE-LUNA, M. T., MAKIELSKI, J. C. & ACKERMAN, M. J. 2007. SCN4B-encoded sodium channel beta4 subunit in congenital long-QT syndrome. *Circulation,* 116**,** 134-42.

MELMAN, Y. F., SHAH, R., DANIELSON, K., XIAO, J., SIMONSON, B., BARTH, A., CHAKIR, K., LEWIS, G. D., LAVENDER, Z., TRUONG, Q. A., KLEBER, A., DAS, R., ROSENZWEIG, A., WANG, Y., KASS, D. A., SINGH, J. P. & DAS, S. 2015. Circulating MicroRNA-30d Is Associated With Response to Cardiac Resynchronization Therapy in Heart Failure and Regulates Cardiomyocyte Apoptosis: A Translational Pilot Study. *Circulation,* 131**,** 2202-16.

MOALI, C., BOUCHER, J. L., SARI, M. A., STUEHR, D. J. & MANSUY, D. 1998. Substrate specificity of NO synthases: detailed comparison of L-arginine, homo-L-arginine, their N omega-hydroxy derivatives, and N omega-hydroxynor-L-arginine. *Biochemistry,* 37**,** 10453-60.

MOHR, A. M. & MOTT, J. L. 2015. Overview of microRNA biology. *Semin Liver Dis,* 35**,** 3-11.

MORAN, A. E., ROTH, G. A., NARULA, J. & MENSAH, G. A. 2014. 1990-2010 global cardiovascular disease atlas. *Glob Heart,* 9**,** 3-16.

MUTHARASAN, R. K., NAGPAL, V., ICHIKAWA, Y. & ARDEHALI, H. 2011. microRNA-210 is upregulated in hypoxic cardiomyocytes through Akt- and p53-dependent pathways and exerts cytoprotective effects. *Am J Physiol Heart Circ Physiol,* 301**,** H1519-30.

NABUURS, C. I., CHOE, C. U., VELTIEN, A., KAN, H. E., VAN LOON, L. J., RODENBURG, R. J., MATSCHKE, J., WIERINGA, B., KEMP, G. J., ISBRANDT, D. & HEERSCHAP, A. 2013. Disturbed energy metabolism and muscular dystrophy caused by pure creatine deficiency are reversible by creatine intake. *J Physiol,* 591**,** 571-92.

NAHRENDORF, M., SPINDLER, M., HU, K., BAUER, L., RITTER, O., NORDBECK, P., QUASCHNING, T., HILLER, K. H., WALLIS, J., ERTL, G., BAUER, W. R. & NEUBAUER, S. 2005. Creatine kinase knockout mice show left ventricular hypertrophy and dilatation, but unaltered remodeling post-myocardial infarction. *Cardiovasc Res,* 65**,** 419-27.

OEMAR, B. S., WERNER, A., GARNIER, J. M., DO, D. D., GODOY, N., NAUCK, M., MARZ, W., RUPP, J., PECH, M. & LUSCHER, T. F. 1997. Human connective tissue growth factor is expressed in advanced atherosclerotic lesions. *Circulation,* 95**,** 831-9.

OHNISHI, H., OKA, T., KUSACHI, S., NAKANISHI, T., TAKEDA, K., NAKAHAMA, M., DOI, M., MURAKAMI, T., NINOMIYA, Y., TAKIGAWA, M. & TSUJI, T. 1998. Increased expression of connective tissue growth factor in the infarct zone of experimentally induced myocardial infarction in rats. *J Mol Cell Cardiol,* 30**,** 2411-22.

OSBOURNE, A., CALWAY, T., BROMAN, M., MCSHARRY, S., EARLEY, J. & KIM, G. H. 2014. Downregulation of connexin43 by microRNA-130a in cardiomyocytes results in cardiac arrhythmias. *J Mol Cell Cardiol,* 74**,** 53-63.

PILZ, S., MEINITZER, A., TOMASCHITZ, A., DRECHSLER, C., RITZ, E., KRANE, V., WANNER, C., BOEHM, B. O. & MARZ, W. 2011a. Low homoarginine concentration is a novel risk factor for heart disease. *Heart,* 97**,** 1222-7.

PILZ, S., TEERLINK, T., SCHEFFER, P. G., MEINITZER, A., RUTTERS, F., TOMASCHITZ, A., DRECHSLER, C., KIENREICH, K., NIJPELS, G., STEHOUWER, C. D., MARZ, W. & DEKKER, J. M. 2014. Homoarginine and mortality in an older population: the Hoorn study. *Eur J Clin Invest,* 44**,** 200-8.

PILZ, S., TOMASCHITZ, A., MEINITZER, A., DRECHSLER, C., RITZ, E., KRANE, V., WANNER, C., BOHM, B. O. & MARZ, W. 2011b. Low serum homoarginine is a novel risk factor for fatal strokes in patients undergoing coronary angiography. *Stroke,* 42**,** 1132-4.

RADOMSKI, M. W., PALMER, R. M. & MONCADA, S. 1990. An L-arginine/nitric oxide pathway present in human platelets regulates aggregation. *Proc Natl Acad Sci U S A,* 87**,** 5193-7.

RIAD, A., JAGER, S., SOBIREY, M., ESCHER, F., YAULEMA-RISS, A., WESTERMANN, D., KARATAS, A., HEIMESAAT, M. M., BERESWILL, S., DRAGUN, D., PAUSCHINGER, M., SCHULTHEISS, H. P. & TSCHOPE, C. 2008. Toll-like receptor-4 modulates survival by induction of left ventricular remodeling after myocardial infarction in mice. *J Immunol,* 180**,** 6954-61.

ROBINSON, R. B. & SIEGELBAUM, S. A. 2003. Hyperpolarization-activated cation currents: from molecules to physiological function. *Annu Rev Physiol,* 65**,** 453-80.

ROMAINE, S. P., TOMASZEWSKI, M., CONDORELLI, G. & SAMANI, N. J. 2015. MicroRNAs in cardiovascular disease: an introduction for clinicians. *Heart,* 101**,** 921-8.

RÖSZER, T. 2012. *The Biology of Subcellular Nitric Oxide*, Springer.

SALEH, M. C., WHEELER, M. B. & CHAN, C. B. 2002. Uncoupling protein-2: evidence for its function as a metabolic regulator. *Diabetologia,* 45**,** 174-87.

SATOH, M., MINAMI, Y., TAKAHASHI, Y., TABUCHI, T. & NAKAMURA, M. 2011. A cellular microRNA, let-7i, is a novel biomarker for clinical outcome in patients with dilated cardiomyopathy. *J Card Fail,* 17**,** 923-9.

SCHROEDER, A., MUELLER, O., STOCKER, S., SALOWSKY, R., LEIBER, M., GASSMANN, M., LIGHTFOOT, S., MENZEL, W., GRANZOW, M. & RAGG, T. 2006. The RIN: an RNA integrity number for assigning integrity values to RNA measurements. *BMC Mol Biol,* 7**,** 3.

SCHULTE, C. & ZELLER, T. 2015. microRNA-based diagnostics and therapy in cardiovascular disease-Summing up the facts. *Cardiovasc Diagn Ther,* 5**,** 17-36.

SIPILÄ, I. 1980. Inhibition of arginine-glycine amidinotransferase by ornithine. A possible mechanism for the muscular and chorioretinal atrophies in gyrate atrophy of the choroid and retina with hyperornithinemia. *Biochim Biophys Acta,* 613**,** 79-84.

SMITH, P. K., KROHN, R. I., HERMANSON, G. T., MALLIA, A. K., GARTNER, F. H., PROVENZANO, M. D., FUJIMOTO, E. K., GOEKE, N. M., OLSON, B. J. & KLENK, D. C. 1985. Measurement of protein using bicinchoninic acid. *Anal Biochem,* 150**,** 76-85.

SPINDLER, M., MEYER, K., STROMER, H., LEUPOLD, A., BOEHM, E., WAGNER, H. & NEUBAUER, S. 2004. Creatine kinase-deficient hearts exhibit increased susceptibility to ischemia-reperfusion injury and impaired calcium homeostasis. *Am J Physiol Heart Circ Physiol,* 287**,** H1039-45.

STOCKLER, S., ISBRANDT, D., HANEFELD, F., SCHMIDT, B. & VON FIGURA, K. 1996. Guanidinoacetate methyltransferase deficiency: the first inborn error of creatine metabolism in man. *Am J Hum Genet,* 58**,** 914-22.

STOCKLER, S., SCHUTZ, P. W. & SALOMONS, G. S. 2007. Cerebral creatine deficiency syndromes: clinical aspects, treatment and pathophysiology. *Subcell Biochem,* 46**,** 149-66.

TEAM, R. D. C. 2008. *R: A language and environment for statistical computing.,* Vienna, Austria, R Foundation for Statistical Computing.

TEN HOVE, M., LYGATE, C. A., FISCHER, A., SCHNEIDER, J. E., SANG, A. E., HULBERT, K., SEBAG-MONTEFIORE, L., WATKINS, H., CLARKE, K., ISBRANDT, D., WALLIS, J. & NEUBAUER, S. 2005. Reduced inotropic reserve and increased susceptibility to cardiac ischemia/reperfusion injury in phosphocreatine-deficient guanidinoacetate-N-methyltransferase-knockout mice. *Circulation,* 111**,** 2477-85.

TOWNSEND, N., WILSON, L., BHATNAGAR, P., WICKRAMASINGHE, K., RAYNER, M. & NICHOLS, M. 2016. Cardiovascular disease in Europe: epidemiological update 2016. *Eur Heart J,* 37**,** 3232-3245.

VACCARI, T., MORONI, A., ROCCHI, M., GORZA, L., BIANCHI, M. E., BELTRAME, M. & DIFRANCESCO, D. 1999. The human gene coding for HCN2, a pacemaker channel of the heart. *Biochim Biophys Acta,* 1446**,** 419-25.

WALLIS, J., LYGATE, C. A., FISCHER, A., TEN HOVE, M., SCHNEIDER, J. E., SEBAG-MONTEFIORE, L., DAWSON, D., HULBERT, K., ZHANG, W., ZHANG, M. H., WATKINS, H., CLARKE, K. & NEUBAUER, S. 2005. Supranormal myocardial creatine and phosphocreatine

concentrations lead to cardiac hypertrophy and heart failure: insights from creatine transporter-overexpressing transgenic mice. *Circulation,* 112**,** 3131-9.

WANG, J. G., MENG, X., HAN, J., LI, Y., LUO, T. G., WANG, J., XIN, M. & XI, J. Z. 2012. [Differential expressions of miRNAs in patients with nonvalvular atrial fibrillation]. *Zhonghua Yi Xue Za Zhi,* 92**,** 1816-9.

WANG, L., SHAH, P. K., WANG, W., SONG, L., YANG, M. & SHARIFI, B. G. 2013. Tenascin-C deficiency in apo E-/- mouse increases eotaxin levels: implications for atherosclerosis. *Atherosclerosis,* 227**,** 267-74.

WANG, T. J., LARSON, M. G., LEVY, D., BENJAMIN, E. J., LEIP, E. P., OMLAND, T., WOLF, P. A. & VASAN, R. S. 2004. Plasma natriuretic peptide levels and the risk of cardiovascular events and death. *N Engl J Med,* 350**,** 655-63.

WONG, L., LEE, K., RUSSELL, I. & CHEN, C. 2007. *Endogenous Controls for Real-Time Quantitation of miRNA Using TaqMan® MicroRNA Assays* [Online]. Available: http://www3.appliedbiosystems.com/cms/groups/mcb_marketing/documents/generaldocuments/cms_044972.pdf [Accessed 25.08.2018, 10:00].

WONG, L. L., WEE, A. S., LIM, J. Y., NG, J. Y., CHONG, J. P., LIEW, O. W., LILYANNA, S., MARTINEZ, E. C., ACKERS-JOHNSON, M. A., VARDY, L. A., ARMUGAM, A., JEYASEELAN, K., NG, T. P., LAM, C. S., FOO, R. S., RICHARDS, A. M. & CHEN, Y. T. 2015. Natriuretic peptide receptor 3 (NPR3) is regulated by microRNA-100. *J Mol Cell Cardiol,* 82**,** 13-21.

WONG, N. & WANG, X. 2015. miRDB: an online resource for microRNA target prediction and functional annotations. *Nucleic Acids Res,* 43**,** D146-52.

WU, W. H., HU, C. P., CHEN, X. P., ZHANG, W. F., LI, X. W., XIONG, X. M. & LI, Y. J. 2011. MicroRNA-130a mediates proliferation of vascular smooth muscle cells in hypertension. *Am J Hypertens,* 24**,** 1087-93.

WYSS, M. & KADDURAH-DAOUK, R. 2000. Creatine and creatinine metabolism. *Physiol Rev,* 80**,** 1107-213.

ZHANG, B., KIROV, S. & SNODDY, J. 2005. WebGestalt: an integrated system for exploring gene sets in various biological contexts. *Nucleic Acids Res,* 33**,** W741-8.

ZHU, Y. & EVANS, M. I. 2001. Estrogen modulates the expression of L-arginine:glycine amidinotransferase in chick liver. *Mol Cell Biochem,* 221**,** 139-45.

# 11 Danksagung

# 12 Lebenslauf

**Lebenslauf wurde aus datenschutzrechtlichen Gründen entfernt.**

# 13 Eidesstattliche Versicherung

Ich versichere ausdrücklich, dass ich die Arbeit selbständig und ohne fremde Hilfe verfasst, andere als die von mir angegebenen Quellen und Hilfsmittel nicht benutzt und die aus den benutzten Werken wörtlich oder inhaltlich entnommenen Stellen einzeln nach Ausgabe (Auflage und Jahr des Erscheinens), Band und Seite des benutzten Werkes kenntlich gemacht habe.

Ferner versichere ich, dass ich die Dissertation bisher nicht einem Fachvertreter an einer anderen Hochschule zur Überprüfung vorgelegt oder mich anderweitig um Zulassung zur Promotion beworben habe.

Ich erkläre mich einverstanden, dass meine Dissertation vom Dekanat der Medizinischen Fakultät mit einer gängigen Software zur Erkennung von Plagiaten überprüft werden kann.


Unterschrift: ....................................................................